國立臺灣大學醫學院腫瘤醫學研究所

博士論文

Graduate Institute of Oncology

College of Medicine

National Taiwan University

Doctoral Dissertation

大腸直腸癌預後學之研究－著重表觀遺傳學和腫瘤微環境之解析

Studies on the Prognostics of Colorectal Cancer－with Emphasis on Epigenetics and Tumor Microenvironment

陳國興

Kuo-Hsing Chen

指導教授：葉坤輝 博士

Kun-Huei Yeh Ph.D

中華民國 112 年 1 月

January 2023

doi:10.6342/NTU202300311

國立臺灣大學博士學位論文
口試委員會審定書

大腸直腸癌預後學之研究－

著重表觀遺傳學和腫瘤微環境之解析

Studies on the Prognostics of Colorectal Cancer－

with Emphasis on Epigenetics and Tumor

Microenvironment

本論文係陳國興君（學號 D04453003）在國立臺灣大學腫瘤醫學研究所完成之博士學位論文，於民國 111 年 12 月 23 日承下列考試委員審查通過及口試及格，特此證明

口試委員：

葉坤輝（簽名）

（指導教授）

陳主奇　　趙毅

范曜宇　　林亮音

陳志宏

所長　葉坤輝（簽名）

doi:10.6342/NTU202300311

誌謝

修習博士學位過程並非一路順遂，其中甘苦點滴在心頭。若是沒有師長、同好及家人的支持，是不可能完成的。

首先我要感謝指導教授葉坤輝教授。從入學開始，我的每項研究計畫都經過葉教授的指導，內容包括研究主題、實驗技術、計畫和論文的撰寫等。葉教授也鼓勵我勇敢地把想法化為行動，例如 CIMP-high 大腸直腸癌危險因子的研究，就是在老師的鼓勵下開始收案。另外也感謝葉教授對於研究計畫執行面上的支持，對於年輕研究者來說是相當重要的。

接下來，我要感謝論文口試委員們：趙毅教授、林亮音教授、莊曜宇教授、徐志宏教授從每年的論文指導委員會開始到口試當天，不斷地給予許多研究和論文寫作的建議。而陳立宗教授在口試時的指導也相當受用。您們的指導使得我的博士論文更加完善。再來則是感謝鄭安理教授。鄭教授是我當腫瘤內科研修醫師時的指導老師。在那個階段鄭教授的教誨讓我們對於癌症研究有了初步的認識，也對於研究生涯有憧憬。鄭教授的許多金玉良言我到現在仍是牢記心中，比如「寫論文是作結論的過程」、「做研究一定要交朋友」、「要 Plan for success」等。另外，我也要感謝這幾年一路上幫忙我的師長朋友們。梁逸歆醫師不管在實驗上和研究思考上都給我很多的指點、許家郎博士在大數據分析上的協助、袁章祖醫師在病理實驗上的幫忙、林本仁醫師和蘇祐立醫師在臨床研究收案上的大力相助。這印證了鄭教授所言「做研究一定要交朋友」。

最後，我要感謝我最重要的家人。我太太、我的兩個寶貝女兒和我的爸媽。我太太為了給兩個女兒最好的成長環境，選擇自己照顧和兼職工作的做法，相當辛苦。我的爸媽也在照顧我女兒的方面幫忙很多。我的女兒們則總是帶給我滿滿的幸福感。家人的陪伴是我能持續研究的重要動力。

doi:10.6342/NTU202300311

論文摘要

CpG 島甲基化表現型(CpG island methylator phenotype) 大腸直腸癌是一種在 DNA 啟動子許多 CpG 島有廣泛性高度甲基化的一種亞型，和許多臨床病理特徵有高度相關，例如：老年、女性、右側大腸癌、*BRAF V600E* 突變和偶發性錯配修復缺陷大腸直腸癌。CpG 島甲基化表現型的預後角色仍存有爭議。為了探究 CpG 島甲基化表現型的預後角色，我們先前針對 450 位大腸直腸癌病人的檢體分析 CpG 島甲基化表現型等生物標記。結果顯示 CpG 島甲基化表現型在早期癌並不是預後因子，但是在第四期的轉移性癌症中，則病人顯著地有較短的存活期。我們也發現在「年輕型」大腸直腸癌(小於 50 歲診斷癌症)中，CpG 島甲基化表現型大腸直腸癌的比率達 14.3%，明顯較西方族群的比例(約 5%)高。

為了進一步驗證 CpG 島甲基化表現型在台灣「年輕型」大腸直腸癌的高發生率，以及探究大腸直腸癌危險因子與台灣 CpG 島甲基化表現型大腸直腸癌的相關性，我們於 2016-2019 年間「前瞻性」收集大腸直腸癌病人的腫瘤檢體、臨床病理資料和大腸直腸癌危險因子。研究結果顯示，小於 50 歲和大於等於 50 歲的病人中各有 15.7% (14/89)和 15.2% (31/204)是 CpG 島甲基化表現型大腸直腸癌。另外，我們也發現 CpG 島甲基化表現型大腸直腸癌在小於 50 歲的病人中，與較多的第四期診斷、*BRAF V600E* 突變、和高身體質量指數 (≥ 27.5 kg/m^2)有相關。在多變相分析中，只有高身體質量指數 (≥ 27.5 kg/m^2)這個危險因子和 CpG 島甲基化表現型在小於 50 歲的大腸直腸癌病人有顯著相關。這結果驗證了在台灣年輕型大腸直腸癌有高比例是 CpG 島甲基化表現型，而且這些腫瘤與高身體質量指數(≥ 27.5 kg/m^2)有顯著相關。

許多研究指出 *BRAF V600E* 突變型在轉移癌與較差的預後有關。我們團隊之前的研究也發現雖同屬腫瘤細胞基因型 *BRAF V600E* 突變型，在「晚期大腸直腸

doi:10.6342/NTU202300311

癌」與存活期較短相關，但在「早期大腸直腸癌」則與預後無關。有鑑於腫瘤微環境中的免疫組成也可以是大腸直腸癌的預後因子，我們假設 *BRAF V600E* 突變的大腸直腸癌腫瘤內免疫組成有預後影響。因為轉移性 *BRAF V600E* 突變大腸直腸癌的免疫組成很少被研究，我們納入 54 個第四期未接受過治療 *BRAF V600E* 突變的轉移性大腸直腸癌的病人，收集他們的檢體和臨床資料。這些檢體的 RNA 被萃取出來後利用 PanCancer Immune Panel (nanoString)進行免疫基因表現分析。我們的研究結果顯示，許多腫瘤內補體基因的表現與病人預後有關。我們也發展出「補體分數」這個工具。「補體分數」高的腫瘤相較於「補體分數」低的腫瘤有較短的疾病無惡化存活期和總存活期。我們發現「補體分數」也與 C4d (一個補體路徑活化的生物標記)染色的強度有顯著正相關，驗證了 RNA 分析的結果。最後，我們發現，「補體分數」與腫瘤微環境中的 M2 型巨噬細胞所代表的基因表現也是有顯著相關性。因為 M2 型巨噬細胞被認為有促進腫瘤生長的作用。這也許是「補體分數」高的腫瘤有比較差的預後的可能原因之一。

綜合以上，我們的研究首次點出東西方大腸直腸癌在 CpG 島甲基化高表現型大腸直腸癌有不同的發生率，也提醒國人適當身體質量指數(< 27.5 kg/m^2)對大腸癌預防的重要性。我們的研究結果亦將有助於未來對於 *BRAF V600E* 突變大腸直腸癌發展新的治療策略。

關鍵字：大腸直腸癌、預後、CpG 島甲基化表現型、身體質量指數、*BRAF V600E* 突變、補體、腫瘤微環境

doi:10.6342/NTU202300311

Thesis Abstract

The CpG island methylator phenotype-high (CIMP-high) subtype of colorectal cancer (CRC) is characterized by widespread hypermethylation in the CpG islands of DNA promoters. Our previous study demonstrated that CIMP-high was not associated with poor prognosis in early-stage CRC but an independent prognostic factor in Stage 4 CRC in a multivariate analysis model. Among patients with early-onset CRC (EOCRC) diagnosed before 50 years old (y/o), the frequency of CIMP-high was 14.3%, significantly higher than that in the Western population (5%). Thus, we collected specimens from patients with CRC and analyzed the clinicopathologic characteristics and CRC risk factors of patients during 2016-2019. We analyzed the tumor's *KRAS*/*NRAS* mutations, *BRAF V600E* mutation, microsatellite instability (MSI), and CIMP. The results revealed that CIMP-high tumors represented 15.7% (14/89) in EOCRC and 15.2% (31/204) in late-onset CRC (LOCRC, diagnosed at 50 y/o or older), respectively. In addition, we observed that in a multivariate analysis, a high body mass index (BMI) of ≥ 27.5 kg/m^2 was significantly correlated with CIMP-high CRC in those younger than 50 yrs. These findings validated that the frequency of CIMP-high CRC in EOCRC is high in Taiwan and demonstrated the significant association between these tumors and a high BMI.

doi:10.6342/NTU202300311

We previously demonstrated the significant prognostic role in late-stage *BRAF V600E* mutant CRC but not in early-stage tumors. We hypothesized that immune contextures in the tumor microenvironment of *BRAF V600E* mutant CRC have prognostic implications in CRC. We enrolled 54 patients with untreated, metastatic microsatellite-stable *BRAF V600E*-mutated CRC and analyzed the expression of immune-related genes in these tumors. The results showed that many complement genes were associated with patient's survival outcomes. We developed a complement score and observed that *BRAF V600E*-mutated CRC with a high complement score was associated with shorter progression-free survival and overall survival compared to that with a low complement score. Finally, we identified that complement scores were significantly associated with M2 macrophage signatures. This may contribute to the phenomenon that tumors with a high complement score are associated with poor survival.

Therefore, our study indicates different incidences of CIMP-high CRC in Eastern and Western populations, and reminds the importance of a proper BMI (<27.5 kg/m^2) for Taiwanese population. The findings in our study could provide insight into developing novel treatments for *BRAF V600E* mutant CRC.

doi:10.6342/NTU202300311

Key words: Colorectal cancer; prognosis; CpG island methylator phenotype; body mass index; *BRAF V600E* mutation; complement; tumor microenvironment

doi:10.6342/NTU202300311

Table of Contents

Oral examination Committee Approval……i

Acknowledgements (誌謝)……ii

Thesis Abstract in Chinese (論文摘要)……iii

Thesis Abstract……v

Table of Contents……viii

List of Figures……x

List of Tables……xii

List of Abbreviations……xiv

Chapter I. Background……1

1.1 The Epidemiology and Carcinogenesis of Colorectal Cancer……1

1.1.1 Carcinogenesis and Epigenetics in Colorectal Cancer……2

1.2 The Prognostics of Colorectal Cancer: Tumor Cells……4

1.3 The Prognostics of Colorectal Cancer: Epigenetics……9

1.4 The Prognostics of Colorectal Cancer: Tumor Microenvironment……11

Chapter II. The Epigenetics of Colorectal Cancer－From Prognostics to Carcinogenesis……14

2.1 Introduction……14

2.2 Methods……15

2.3 Results……20

2.4 Discussion……22

Chapter III. The Study of Tumor Microenvironment in Metastatic BRAF V600E mutant Colorectal Cancer……27

3.1 Introduction……27

doi:10.6342/NTU202300311

3.2 Methods……..…..29

3.3 Results……..…..36

3.4 Discussion……..41

Chapter IV. Conclusion and Future Perspectives……..…..46

4.1 Prognostics, Carcinogenesis, Epigenetics and Microbiome……..46

4.2 Prognostics, Tumor Microenvironment, and Complement Activation……....47

4.3 Prognostics: Open the Door to Future Colorectal Cancer Researches……..50

Chapter V. Figures……..….54

Chapter VI. Tables……. ……..……...69

References……...……86

Appendix……...103

doi:10.6342/NTU202300311

List of Figures

Figure 1. Age-adjusted incidence rates (ASR) of colorectal cancer (ICD 10 codes C18-C20) for both gender in Taiwan using the WHO standard population 2000……...54

Figure 2. Flow chart of patient enrollment in this study…….55

Figure 3. The survival probability in patients with *de novo* metastatic MSS *BRAF V600E* mutant CRC by Kaplan–Meier analysis…….…….....56

Figure 4. The prognostic implication of complement genes expression……57

Figure 5. The prognostic implication of complement genes expression……59

Figure 6. The prognostic values of complement score……...61

Figure 7. The correlation between complement score and the specific metastatic sites……...…...63

Figure 8. The survival probability by Kaplan–Meier analysis in patients with low and high complement scores……..……..…..64

Figure 9. The survival probability by Kaplan–Meier analysis in patients with a high complement score compared with those with a low complement score in TCGA dataset. ……65

Figure 10. The correlation of the complement score and C4d density in *de novo*

doi:10.6342/NTU202300311

metastatic MSS *BRAF V600E* mutant CRC…...……...67

Figure 11. The analysis of immune cell abundance revealed a strong association between the complement score and M2 macrophages……68

doi:10.6342/NTU202300311

List of Tables

Table 1. The primers used for CpG Island Methylator Phenotype testing in MethyLight study…….……69

Table 2. Distribution of CIMP-high or CIMP-low/negative according to clinicopathologic variables. Logistic regression was used for statistical analysis……..70

Table 3. Distribution of CIMP-high or CIMP-low/negative according to clinicopathologic variables stratified by age. Chi-square test, and Fisher's exact test were used for statistical analysis……72

Table 4. Distribution of CIMP-high or CIMP-low/negative according to risk factors of CRC in overall patients and stratified by age. Logistic regression was used for statistical analysis……...….74

Table 5. Multivariate analysis for the association between CIMP-high CRC and clinicopathological variables in overall patients, patients with age < 50y and age ≥ 50y……...……76

Table 6. Distribution of CIMP-high or CIMP-low/negative according to clinicopathologic variables stratified by gender. Chi-square test, and Fisher's exact test

doi:10.6342/NTU202300311

were used for statistical analysis……77

Table 7. Distribution of CIMP-high or CIMP-low/negative according to risk factors of CRC stratified by gender. Logistic regression was used for statistical analysis…….78

Table 8. Clinicopathological features in patients with *BRAF V600E*-mutated colorectal cancer……..…….80

Table 9. Immune cells in Cox proportional hazard model for hazard ratios of progression-free survival and overall survival in patients with *de novo* metastatic MSS *BRAF V600E*-mutated CRC……...…….81

Table 10. Immune checkpoints link to B and T cell signaling in Cox proportional hazard model for hazard ratios of progression-free survival and overall survival in patients with *de novo* metastatic MSS *BRAF V600E*-mutated CRC……...……82

Table 11. Complement genes in the Cox proportional hazards model for hazard ratios of progression-free survival and overall survival in patients with *de novo* metastatic MSS *BRAF V600E* mutant CRC……...…..83

Table 12. Univariate and multivariate analyses through a Cox proportional hazards model for hazard ratios of progression-free survival and overall survival in patients with *de novo* metastatic MSS *BRAF V600E* mutant CRC……...84

doi:10.6342/NTU202300311

List of Abbreviations

ASR	Age-adjusted incidence rate
BMI	Body mass index
BM	*BRAF* mutant classification
CI	Confidence interval
CIMP	CpG island methylator phenotype
CMS	Consensus molecular subtypes
CRC	Colorectal cancer
DM	Diabetes mellitus
DMG	Differentially methylated gene
dMMR	Mismatch repair deficiency
EOCRC	Early-onset colorectal cancer
FFPE	Formalin-fixed paraffin embedded
HDI	Human Development Index
HR	Hazard ratio
HRT	Hormone replacement therapy
IBD	Inflammatory bowel disease

doi:10.6342/NTU202300311

KCGMH	Kaohsiung Chang Gung Memorial Hospital
LOCRC	Late-onset colorectal cancer
MSI-high	Microsatellite instability-high
MSS	Microsatellite stable
NSAID	Non-steroidal anti-inflammatory drug
NTUH	National Taiwan University Hospital
NTUH-iMD	National Taiwan University Hospital-integrated Medical Database
ORR	Objective response rate
OS	Overall survival
PFI	Progression-free interval
PFS	Progression-free survival
PMR	Percentage of methylated reference
TAM	Tumor-associated macrophage
TCGA	The Cancer Genome Atlas
TME	Tumor microenvironment
TLS	Tertiary lymphoid structure

doi:10.6342/NTU202300311

Chapter I. Background

1.1 The Epidemiology and Carcinogenesis of Colorectal Cancer

Globally, colorectal cancer (CRC) ranks third in cancer incidence and second in cancer mortality[1]. There were estimated more than 1.9 million new CRC cases and 930,000 deaths due to CRC in 2020. CRC is more common in countries with very high/high Human Development Index (HDI) than those with low/medium HDI. The highest incidence of CRC is noted in European countries, Northern America, Australia, and New Zealand followed by Eastern Asia. CRC incidence is still increasing steadily in most countries but has declined for years in the United States, Canada, Australia, and New Zealand, probably related to different screening programs[2]. In Taiwan, CRC incidence has increased in the past 30 years, and CRC has been the leading type of cancer in newly diagnosed cases for more than 14 years (Figure 1)[3,4]. In 2019, more than 17,000 patients were diagnosed with CRC, among whom 6,400 died.

Based on epidemiologic studies, risk factors of CRC include family histories of patients with CRC, inflammatory bowel disease (IBD), diabetes mellitus (DM), obesity, sedentary lifestyle, cigarette smoking, and excessive consumption of red meat and alcohol [5]. These risk factors may present together and have different relative risks for

doi:10.6342/NTU202300311

CRC. The highest relative risk is related to the histories of patients with CRC in their first-degree relatives and people with IBD (relative risk more than 2). Taylor et al. analyzed a population-based resource with 2,327,327 people included in three or more generations of family histories[6], among whom 10,556 had CRC. The relative family risk for CRC in those with affected first-degree relatives was 2.05. Jess et al. performed a meta-analysis of 8 population-based studies to calculate the relative risk of CRC in patients with ulcerative colitis (UC)[7]. They demonstrated that UC increases the risk of CRC up to 2.4 folds. Other risk factors are generally modifiable and contribute to lower relative risk (mostly between 1.2-2.0) but are associated with a bigger disease burden in the world[5].

1.1.1 Carcinogenesis and Epigenetics in CRC

Many risk factors, such as DM and obesity, are associated with metabolic dysregulation attributed to aberrant epigenetic regulation of gene expression, which can be adaptive and responsive to environmental exposures[8]. In the Dutch Hunger Winter cohort, the investigators recruited the residents who experienced World War II in different regions of Dutch and followed up on the development of cancer[9]. The individuals who lived in the Western urban regions experienced the highest energy

doi:10.6342/NTU202300311

restriction (rationing < 700 kcal per day, 1944-45) in their childhood; their adolescence was associated with less CRC incidence than those in other regions. The molecular subtype that was substantially decreased in CRC incidence was CpG island methylator phenotype (CIMP), which was characterized by diffuse hypermethylation in CpG island throughout the genomes[10]. One study analyzed genome-wide methylation in the whole blood of two groups of baboons living in different areas and having different resources (wild feeding vs. lodge feeding). Famine exposure was associated with the most differentially methylated regions in the key gene, phosphofructokinase platelet (*PFKP*), in the glycolysis pathway between these two groups of baboons[11]. Inspired by these two studies, we collected CRC tumors and the adjacent normal colon tissues and analyzed their differentially methylated genes (DMGs) by genome-wide methylation array. We focused on the genes in the glycolysis pathway and compared our results to three open datasets: GSE42752, GSE25062, and the Cancer Genome Atlas (TCGA). We found that multiple loci were involved in Hexokinase containing domain 1 (*HKDC1*) (hypomethylation) and Aldehyde dehydrogenase 1 family member A3 (*ALDH1A3*) (hypermethylation)[12]. The results warrant further study to explore the roles of these two DMGs in CRC development.

doi:10.6342/NTU202300311

1.2 The Prognostics of CRC: Tumor Cells

CRC is a heterogeneous disease associated with many genetic and epigenetic alterations. Among these molecular alterations, some have prognostic implications. The common examples of molecular prognostic markers in CRC are listed below.

***KRAS* and *NRAS* mutation**

The RAS-RAF-MEK-ERK pathway is one of the most common deregulated pathways in human cancers[13]. It mediates many important cellular signals, such as growth, proliferation, and senescence. Activating *RAS* point mutations could activate the RAS-RAF-MEK-ERK pathway and occur in about 30% of human cancers[14]. There are three human *RAS* genes: *KRAS*, *NRAS*, and *HRAS.* According to several studies, mutations in *KRAS* exon 2-4 and *NRAS* exon 2-4 accounted for 50% of metastatic CRC and were both negative predictors for the efficacy of anti-EGFR antibody[15-17]. *RAS* mutations also have prognostic implications in metastatic CRC. In the TRIBE study, which compared the combination of bevacizumab and FOLFOXIRI and the combination of bevacizumab and FOLFIRI as the first-line treatment in metastatic CRC, the median overall survival (OS) in the group of patients with *RAS* mutant was shorter than that in the group of patients with *RAS*/*BRAF* wild type [18]. In another study,

doi:10.6342/NTU202300311

Modest et al. performed a pooled analysis of five randomized clinical trials and enrolled 1,239 patients with metastatic CRC, among whom 462 patients had *KRAS* mutations, 39 had *NRAS* mutations, and 74 had *BRAF* mutations. Patients with *KRAS* mutations had significantly shorter OS and progression-free survival (PFS) than those with *RAS*/*BRAF* wild-type tumors[19]. Tumors with *KRAS G12C* and *KRAS G13D* were significantly correlated with shorter OS than tumors with *RAS*/*BRAF* wild type, and *KRAS G12D* and *KRAS G12S* did not have a prognostic association. The prognostic roles of *NRAS* mutations are still controversial. *NRAS* mutations in tumors had no significant prognostic impact in Modest's study but were associated with shorter OS compared to the wild-type *NRAS* in tumors in another study[19,20].

***BRAF* mutation**

BRAF is also involved in the RAS-RAF-MEK-ERK pathway[21]. Mutant BRAF proteins contribute to elevated kinase activity independent of the upstream RAS signaling. Somatic *BRAF* mutations in human cancers were first reported in 2002, and in that report, *BRAF* mutations accounted for 12% of CRC[21]. *BRAF* mutations represent about 4.7–8.7% of metastatic CRC; this type of tumor is significantly associated with more proximal colon cancer, high microsatellite instability, peritoneal metastases, and

doi:10.6342/NTU202300311

distal lymph node metastases but fewer lung metastases[22-24]. Many studies reported that *BRAF* mutations significantly predicted poor survival in patients with metastatic CRC, and those with *BRAF* mutant CRC had a median OS of 11–14 months[23,24]; *V600E* mutation was the most frequent and contributed to poor prognosis. Non-*V600E BRAF* mutations accounted for 2.2% of metastatic CRC, and patients with non-*V600E BRAF* mutations had an excellent prognosis[25]. In Taiwan, Tsai et al. reported that there was a high frequency (11/59, 19%) of *BRAF V600E* mutations in very young patients (< 30 y/o) with CRC and patients with *BRAF V600E* mutations had shorter survival than patients with wild type *BRAF*[26]. Our team previously demonstrated that *BRAF* mutations had a paradoxical role in the prognosis of the early and late stages of CRC[27]. In the late stage of CRC, *BRAF V600E* mutation was an independent prognostic factor, while in the early stage of CRC, *BRAF V600E* mutation had no impact on prognosis. The mechanism contributed to the paradoxical role in the prognosis of different stages of CRC with the *BRAF V600E* mutation is unknown. We hypothesize that the immune contexture in the tumor microenvironment (TME) may play an important role. The prognostic implication of the immune contexture in TME will be described in detail in the next section.

doi:10.6342/NTU202300311

Mismatch repair deficiency and microsatellite instability-high

Mismatch repair deficiency (dMMR) represents defects in DNA mismatch repair function due to germline mutations or hypermethylation of one of the mismatch repair genes (*MLH1*, *PMS2*, *MSH2*, *MSH6*)[28]. CRC with dMMR is characterized by many insertion and deletion mutations in the genome and a high mutational burden[29,30]. Microsatellite instability-high (MSI-high) is a genetic fingerprint of dMMR, Generally detected by the loss of expression of mismatch repair proteins in immunohistochemical stains. MSI-high is determined by PCR amplification of the Bethesda panel, which consists of five microsatellite loci (two mononucleotides and three dinucleotides), or the Promega panel, which includes five mononucleotides. Clinically, MSI-high CRC represents about 15% of CRC, and patients with MSI-high CRC have a better prognosis than those with microsatellite stable (MSS) CRC[31,32]. Gryfe and colleagues also demonstrated that MSI-high CRC was associated with less frequent regional lymph nodes and distant organ metastases than MSS CRC[31]. A meta-analysis of the prognostic impact of MSI-high in CRC enrolling 32 clinical studies and 7,642 patients with CRC (1,277 patients with MSI-high CRC); it demonstrated that MSI-high was an independent factor for a favorable prognosis[32]. The underlying mechanism for patients

doi:10.6342/NTU202300311

with MSI-high CRC having a better prognosis than those with MSS CRC is still undefined. One mechanism might be due to the fact that more immunoreactive cells infiltrated in the TME of MSI-high tumors than in MSS tumors[33,34].

Recently, dMMR was identified as a predictive biomarker for anti-PD-1 antibodies in metastatic CRC and other cancer types. Le et al. reported that in patients with dMMR CRC, the objective response rate (ORR) for anti-PD-1 antibody was 40% (4/10), but there was no responder in the group with proficient mismatch repair CRC (0/18, 0%). In addition, the ORR was also high (4/7, 57%) in CRC with non-dMMR [35]. Other studies further supported the predictive role of dMMR in response to anti-PD-1 antibodies in metastatic CRC and other cancers[36,37]. These results led to the FDA approval of pembrolizumab and nivolumab to treat metastatic dMMR/MSI-high CRC and pembrolizumab as a tissue/site agonistic therapy in metastatic dMMR or MSI-high solid tumors[38]. A further randomized controlled study proved that pembrolizumab was superior to the standard of care in first-line therapy for metastatic CRC with dMMR/MSI-high[39]. The high response of anti-PD-1 therapy in dMMR or MSI-high tumors may be attributed to high indel mutational load, increased neoantigens amount, DNA sensing, and vigorous infiltrative CD8+ T cells [35,36,40,41]. Recently, anti-PD-1

doi:10.6342/NTU202300311

antibodies with and without an anti-CTLA4 antibody were investigated in nonmetastatic CRC, and the results also showed favorable clinical and pathological response rates[42,43].

1.3 The Prognostics of CRC: Epigenetics

In addition to genetic alterations, some studies also revealed that epigenetic alterations might be prognostic factors[44]. CIMP-high is one of the common epigenetic alterations reported as a prognostic factor.

CIMP

CIMP-high CRC was originally recognized by Toyota and colleagues in 1999. They used methylated CpG island amplification to identify several cancer-specific clones (type C methylation)[45] and identified a subgroup of CRC with a high level of type C methylation; those tumors were characterized by proximal colon cancer and MSI-high. Thus, a new pathway in CRC was identified, and a new CRC carcinogenesis, mixed with genetic alterations and inactivation of tumor suppressor genes by hypermethylation, was proposed[46]. During the following years, several panels were developed to determine CIMP-high CRC, including the classic panel (*MINT1*, *MINT2*, *MINT31*, *p16*, and *MLH1*), Weisenberger's panel (*CACNA1G, IGF2, NEUROG1, RUNX3*, and *SOCS1*), and others[47-50]. Although these studies used different panels, they

doi:10.6342/NTU202300311

revealed common clinicopathologic features of CIMP-high CRC: old age, female, proximal colon cancer, *BRAF V600E* mutation, and MSI-high. Recently, a methylation array was used to classify CIMP CRC and showed that CIMP-high CRC was enriched in hypermutated tumors, probably due to the overlap of hypermutated tumors and MSI-high tumors[29].

The prognostic role of CIMP in CRC has been extensively investigated, but the results were inconsistent[51,52]. Several confounding factors exist in previous studies: first, the overlap of the other prognostic factors with CIMP-high, such as MSI-high and *BRAF V600E* mutation; second, the contribution of anti-cancer therapy to prognosis; finally, a paradoxical role in prognosis with a molecular marker. For example, we previously demonstrated that *BRAF V600E* mutation had a paradoxical role in the early and late stages of CRC[27]. Thus, we investigated the prognostic role of CIMP in different stages (Stages 1-4) of CRC in a retrospective cohort[53]. We performed multivariate analysis to adjust the prognostic effects of molecular factors and anti-cancer therapies. The results revealed that in patients with Stage 1-3 CRC, CIMP-high did not predict poor prognosis; however, in those with Stage 4 CRC, CIMP-high was significantly associated with shorter survival. The impact of CIMP-high was still significant in a

doi:10.6342/NTU202300311

multivariate analysis. Thus, we concluded that CIMP-high was an independent prognostic marker for Stage 4 CRC.

1.4 The Prognostics of CRC: TME

In addition to genetic and epigenetic alterations, immune contexture in TME has a prognostic role in many types of cancer[54,55]. The immune contexture consists of many types of immune cells, chemokines, cytokines, and special structures, such as tertiary lymphoid structure (TLS). TLS is an ectopic lymphoid aggregate adjacent to the tumor bed. It contains B cells, follicular helper T cells, and follicular dendritic cells and is usually generated during chronic inflammation. The study of immune contexture includes the analysis of the density, location, and functions of different types of immune cells through histopathologic or bioinformatic tools. During the past two decades, the clinical impact of immune contexture has been extensively investigated, and the results are quite diverse in different types of immune cells. For example, CD8+T cells and TLS are commonly correlated to good prognosis; in contrast, Treg cells and M2 macrophages are associated with poor prognosis in many cancer types[54].

Pages et al. first showed the infiltrating memory CD45RO+ cells were negatively associated with early metastatic invasions and advanced stages of CRC and survival of

doi:10.6342/NTU202300311

patients with this disease[56]. Then Galon and colleagues found that tumors with Th1 adaptive immunity (CD3, CD8, GZMB, and CD45RO) had a favorable prognosis[57]. Combination analysis of the type, density, and location of these immune cells and their associated molecules had a prognostic value that was independent to and superior to the UICC-TNM stage. These findings led to the development of the immunoscore, which was determined by the density of CD3+ and CD8+ T cells at the core and the invasive front of the tumor[58]. The scoring system ranges from low (Immunoscore 0) to high (Immunoscore 4). Many studies demonstrated that immunoscore outperformed the TNM stage in predicting PFS and OS in early-stage CRC[58-60]. In addition to CD8+ T cells, many other immune cells have been reported to be a good prognostic factor in CRC, such as Th1 cells, Tfh cells, B cells, NK cells, and TLS, and M2 tumor-associated macrophages (TAMs) are correlated to a poor prognosis[55,61-63]. Understanding the impact of immune contexture on clinical outcomes may provide insight into developing novel treatments for CRC.

Our previous study identified that CIMP-high was correlated to a poor prognosis of CRC, and the frequency of CIMP-high tumors (14.7%) in early-onset CRC (EOCRC, diagnosed at age < 50 y/o) seemed to be higher than that in Western populations (5%).

doi:10.6342/NTU202300311

Thus, in this study, we are interested in the actual frequency and risk factors of CIMP-high CRC in Taiwan. Additionally, we demonstrated that *BRAF V600E* mutation predicted a poor prognosis in late-stage CRC. Because immune contexture is a prognostic factor in CRC, they may have prognostic implications in *BRAF V600E* mutant CRC. Thus, we hypothesize that immune contexture in TME of metastatic *BRAF V600E*-mutated CRC is a prognostic factor. In the following two chapters, we focus on these two research topics.

doi:10.6342/NTU202300311

Chapter II. The Epigenetics of CRC－From Prognostics to Carcinogenesis

2.1 Introduction

CIMP-high CRC accounts for 15-20% of all CRC and is characterized by a wide range of DNA hypermethylation in many promoter CpG islands[50]. This type of CRC is associated with clinicopathologic features, such as old age, female, proximal colon cancer, MSI-high, and *BRAFV600E* mutation, and shorter survival in metastatic disease[47,53,64]. The etiology of CIMP-high needs to be clearly defined, but its crosstalk with environmental factors and epigenetic alterations has been well studied[8,65]. Thus, understanding the risk factors of CIMP-high CRC is important. The risk factors of CIMP-high CRC have been studied in Western populations. Weisenberger and colleagues analyzed the associations among CIMP-high genotype, risk factors, and clinicopathologic variables in the Colon Cancer Family Registry cohort that recruited patients with CRC from USA, Canada, and Australia. The results showed that the use of non-steroidal anti-inflammatory drugs (NSAIDs) was significantly associated with CIMP-high CRC in all patients, and smoking and obesity were correlated with CIMP-high CRC only in female patients[64]. However, a relationship between CIMP-high CRC and risk factors in an East Asian population remains to be investigated.

In our previous cohort, we found that the frequency of CIMP-high CRC was 16.4% (N=450), which was in the similar range of the frequency reported in Western populations[53]. However, in Taiwan, the frequency of CIMP-high CRC in EOCRC (14.7%) seemed to be higher than that in the Western populations (5%). Lui et al. also

doi:10.6342/NTU202300311

described that CIMP-high tumors accounted for 17.9% of EOCRC in a Chinese cohort[66]. Both studies indicate that CIMP-high CRC was not associated with old age[53,66].

On the other hand, studies indicate that methylations could be adaptive to environmental exposures[8]. The baboon study and Dutch Hunger Winter study proved that methylations were changed after exposure to famine[10,11]. Thus, we hypothesized that a high frequency of CIMP-high tumors in EOCRC in Taiwan, and those CIMP-high tumors were associated with environmental factors, such as body mass index (BMI). Therefore, we initiated a prospective cohort study to enroll patients diagnosed with CRC in 2016 to prove our hypotheses.

2.2 Methods

Patient eligibility

The target number of recruited patients with CRC was 320, and more than 30% should be EOCRC. Patients who met the following inclusion criteria were eligible for this study: (1) age ≥ 20 y/o, (2) cytologically or pathologically proven CRC and adequate staging (American Joint Cancer Committee on Cancer, 7th edition) by computed tomography, and (3) undergoing a colectomy surgery. The exclusion criteria

doi:10.6342/NTU202300311

were that they received systemic chemotherapy or radiotherapy before colectomy. Written informed consent was obtained from all patients before collecting the tumor specimens. We also collected the patients' clinical and pathological characteristics, including age, sex, histology and grade of tumors, tumor location, the risk factors of CRC, and BMI. The definition of these clinicopathologic variables is described below. For age, the patients were categorized as age < 50 y/o and age ≥ 50 y/o. The histology of tumors included the presence or absence of mucinous components, signet-ring cells, and medullary histology, which were observed by microscopic examination. Mucinous carcinoma was designated if more than 50% of the tumor volume was a mucinous component. The tumor grade was classified into low and high grades. Tumors were graded as a low grade if ≥ 95% of the tumor has glandular formation or MSI-high. Otherwise, tumors were graded as a high grade. Tumor location was grouped into right-sided and left-sided. Right-sided tumors were designated if the primary tumors were located from the cecum to the splenic flexure of the transverse colon, and left-sided tumors were located from descending colon to the rectum. The Institute Review Board of National Taiwan University Hospital (NTUH) approved this study.

Risk factors

doi:10.6342/NTU202300311

In this study, risk factors include first-degree family history for CRC, history of colorectal polyp, DM, hyperlipidemia, BMI at diagnosis, pre-diagnosis use of NSAIDs, and hormonal replacement therapy (HRT). These data were obtained from interviews with the patients and the survey of the electronic chart of NTUH. The definitions of these risk factors are described below. Patients with more than one first-degree family member diagnosed with CRC were grouped into a group with a family history of CRC. BMI at diagnosis was retrieved from a medical record. We categorized BMI into three groups based on WHO criteria of 18–24.9, 25–29.9, and ≧30 kg/m^2. We also categorized BMI into two groups (< 27.5 and ≧ 27.5 kg/m^2) according to the experts' opinion for appropriate BMI in Asian populations from WHO expert consultation[67]. In that report, a BMI of ≧ 27.5 kg/m^2 was regarded as a high risk for public health. Histories of DM and hyperlipidemia were determined according to self-reports and/or the identification of the use of medication for these diseases. Pre-diagnosis NSAIDs use was defined if two or more times per week in one month or longer within one year of NSAIDs use was reported. Pre-diagnosis of HRT use was determined if six months or longer of HRT use within one year was reported.

CIMP analysis

doi:10.6342/NTU202300311

We used a QIAamp DNA formalin-fixed paraffin-embedded (FFPE) tissue kit to extract genomic DNA from tumor specimens (Qiagen, Santa Clarita, CA, USA). Then the genomic DNA was treated with sodium bisulfide according to the EZ DNA Methylation Kit protocol (Zymo Research, Irvine, CA, USA). We evaluated the methylation status of five loci: *MINT1*, *MINT2*, *MINT31*, *p16*, and *MLH1* (classical panel) using MethyLight assay, which was a probe-based, methylation-specific real-time polymerase chain reaction technology. The primers used for the MethyLight study are listed in Table 1. The methylation-independent *Alu* repeat was measured for normalization control reaction. The methylation levels of five loci in tumor samples and a constant reference sample were measured, and quantification analysis of DNA methylation was performed. The percentage of methylated reference (PMR) of each locus was calculated based on the equation proposed in a previous study as the following: PMR = 100 × (methylated reaction / control reaction)$_{sample}$ / (methylated reaction / control reaction)$_{M.SssI\text{-}Reference}$. A PMR of > 10 was regarded as hypermethylated[49]. Finally, CIMP-high tumors were determined if there were three or more loci with a PMR of >10 identified. Otherwise, the tumors were determined as CIMP-low/negative.

doi:10.6342/NTU202300311

RAS/*BRAF* mutation analysis

We evaluated *RAS* (*KRAS* and *NRAS*) and *BRAF* mutations by PCR coupled with Sanger's sequencing method. The primers in this study covered exons 2, 3, and 4, including codons 12, 13, and 61 of *KRAS* and *NRAS*, and covered exon 15 of *BRAF*. After PCR, we used an automated ABI 3730 sequencer (Applied Biosystems, Foster City, CA, USA) for direct sequencing.

MSI analysis

We used the MSI Analysis System (Promega Corp., Madison, WI, USA), a PCR-based assay for detecting MSI, in five mononucleotide loci (NR-21, NR-24, MONO-27, BAT-25, and BAT-26). Tumors were designated MSI-high if abnormal allele length was identified in two or more loci. Otherwise, tumors were MSS.

Statistical analysis

The patient's clinicopathological characteristics were presented as percentages and frequencies. The association between CIMP-high CRC and clinicopathological variables was estimated by logistic regression (Table 2), Fisher's exact test, and Chi-square test (Table 3 and Table 6). The association between risk factors and CIMP-high CRC was also evaluated by logistic regression (Table 4 and Table 7). Finally, we used a

doi:10.6342/NTU202300311

multivariate logistic regression model to evaluate the odds ratio of each variable for CIMP-high tumors. Only a 2-sided *p*-value of ≤ 0.05 was considered statistically significant. Only the variables with a *p*-value less than 0.1 in univariate analysis (Table 3 and Table 4) were put into a multivariate logistic regression model. All the statistical analyses were performed using SAS statistical software (version 9.4, SAS Institute, Cary, NC, USA).

2.3 Results

From March 2016 to June 2019, we enrolled 320 patients, among whom 99 (30.9%) were younger than 50 y/o. The clinicopathological characteristics of these tumors and the risk factors of CRC were well-collected. Among collected tumor samples, 293 (91.6%) had enough genomic DNA for CIMP analysis, and 288 (90%), 286 (89.4%), and 318 (99.4%) were adequate for *RAS* mutation, *BRAF V600E* mutation, and MSI analyses, respectively. Finally, 293 tumors were enrolled in the primary analysis, among which 89 (30.4%) were EOCRC.

In the primary analysis, CIMP-high CRC accounted for 15.4% of all CRC. The frequencies of CIMP-high CRC in patients aged < 50 y/o and aged ≥ 50 y/o were 15.7% (14/89) and 15.2 % (31/204), respectively. The distribution of CIMP-high and CIMP-

doi:10.6342/NTU202300311

low/negative tumors in clinicopathological variables is presented in Table 2. The key findings are described briefly here. CIMP-high CRC was significantly associated with *BRAF V600E* mutation ($p < 0.01$), MSI-high genotype ($p < 0.01$), and right-sided primary tumor ($p = 0.03$). In contrast, it was not associated with gender ($p = 0.49$) and old age ($p = 0.91$). Then we further evaluated the distribution of CIMP-high and CIMP-low/negative tumors in clinicopathological variables in two age groups (age < 50 y/o and age ≥ 50 y/o), and the results are shown in Table 3. In EOCRC, CIMP-high tumors were significantly associated with *BRAF V600E* mutation ($p < 0.01$) and stage IV at diagnosis ($p < 0.01$). In contrast, CIMP-high tumors were significantly associated with right-sided primary tumor ($p = 0.02$), *BRAF V600E* mutation ($p < 0.01$), and MSI-high ($p < 0.01$) in late-onset CRC (LOCRC, diagnosed at age ≥ 50 y/o).

The distributions of CIMP-high and CIMP-low/negative CRC associated with various risk factors in overall patients and patients aged < 50 y/o and aged ≥ 50 y/o are shown in Table 4. In patients younger than 50 yrs, CIMP-high CRC was likely associated with a BMI of ≥ 27.5 kg/m^2 ($p = 0.09$). In contrast, in those 50 yrs or older, CIMP-high CRC was significantly associated with colorectal polyp ($p = 0.03$). In the multivariate logistic regression model, we found BMI of ≥ 27.5 kg/m^2 ($p = 0.03$) and

doi:10.6342/NTU202300311

Stage 4 disease at diagnosis ($p < 0.01$) were independent factors for early-onset CIMP-high CRC; however, only MSI-high ($p < 0.01$) was an independent factor for late-onset CIMP-high CRC (Table 5). We also performed the statistical analysis of CIMP-high CRC, clinicopathological features, and risk factors by gender, and the results are presented in Tables 6 and 7, respectively.

2.4 Discussion

In this prospective study, we showed that the high frequency (15.7%) of CIMP-high CRC in EOCRC was consistent with the result from our previous study (14.3%, 11/77)[53]. These findings might not be related to the classical panel because a similar frequency of CIMP-high genotype (17.9%) in EOCRC was found in a Chinese cohort, and CIMP-high tumors were determined by ≥ 3/5 of the Weisenberger's panel in that study[66]. In addition, one study demonstrated no significant difference between these two panels in the correlation to clinicopathological features[68]. Thus, there may be different frequencies of CIMP-high tumors in EOCRC between East Asian and Western populations; this warrants further large-size studies to confirm this molecular epidemiology difference.

In addition to the frequency of CIMP-high CRC, we also found significant

doi:10.6342/NTU202300311

associations between CIMP-high CRC and *BRAF V600E* mutation, MSI-high, right-sided primary tumor, or stage 4 at diagnosis. These findings are consistent with previous analyses[53,64,69]. We demonstrated that CIMP-high CRC had no association with old age and females, different from the data from Western populations. Moreover, we showed different associations among risk factors, clinicopathological features, and a CIMP-high genotype in EOCRC and LOCRC. In multivariate analysis, a BMI of ≥ 27.5 kg/m^2 was the only independent risk factor for CIMP-high CRC in patients younger than 50. The WHO expert consultation had added the thresholds of 23, 27.5, 32.5, and 37.5 kg/m^2 for the operation of public health in Asian populations in 2004 because the prevalence of cardiovascular diseases and type II DM were increased and the average BMI in these populations was below 25 kg/m^2[67]. People with a BMI of ≥ 27.5 kg/m^2 represented the high-risk groups. Our study indicates the importance of maintaining an adequate BMI, especially in people younger than 50. In Weisenberger's study, the investigators did not evaluate the association between risk factors and CIMP-high CRC in different age groups. Still, they found a higher BMI was significantly associated with CIMP-high CRC in female patients[64]. However, our study did not identify this association (Table 7). So further study is needed to clarify these controversial findings.

doi:10.6342/NTU202300311

Why was CIMP-high CRC significantly correlated to a high BMI in younger patients? An analysis of the Dutch Hunger Winter cohort revealed that early-life exposure to famine was significantly associated with decreased incidence of CRC, specifically, the CIMP-high CRC[70]. In an animal model, the caloric restriction could delay methylation drift during aging[71]. Thus, the correlation between a high BMI and CIMP-high CRC may be related to calorie overload-induced biologic effects. On the other hand, epigenetic aging may also play a role. Epigenetic aging is proposed to be the accumulating work done by an epigenetic maintenance system[72]. Epigenetic aging can be evaluated by genome-wide DNA methylation array, and accelerated epigenetic aging is associated with CRC, especially CIMP-high CRC[73]. Obesity also accelerates epigenetic aging in multiple kinds of human tissues[72,74]. Thus, the excessive accumulated aging-related methylations in obese or overweight patients may contribute to hypermethylated cancers. The next question is why the significant association between CIMP-high CRC and high BMI was only observed in younger patients aged < 50 y/o but not in older patients aged ≥ 50 y/o. A recent report provided potential explanations. Nevalainen's study showed the correlation of an increased BMI with accelerated epigenetic age only in middle-aged individuals (40-49 y/o) but not in

doi:10.6342/NTU202300311

young-aged (15-24) and very old (> 90 y/o) individuals[75]. Instead, they observed a high BMI was correlated with a lower epigenetic age in very old individuals. Based on these findings, we hypothesize that a higher BMI accelerates epigenetic aging, and it should have a long enough time to let obesity-induced epigenetic aging contribute to CRC in patients with middle age. But for older patients with CRC with a high BMI, the etiology may be different because they have more time (chances) to acquire multiple epigenetic and genetic alterations, so obesity-induced accelerated aging has less influence.

There are several limitations in the present study. First, the sample size is relatively small, which may confound the results of the associations between CIMP-high CRC and variables in different age and gender groups. Second, we lack reliable data on smoking and alcohol consumption and could not explore the association between them and CIMP-high CRC. Many studies indicate the dose-dependent relationship between smoking and CIMP-CRC, so the absence of the smoking analysis would be influential[64,69]. Regarding the association between alcohol consumption and CIMP-high CRC, the results were conflicting[64,76]. This study has strengths. This study is a prospective cohort study, so we can easily collect clinical data and risk factors like BMI. Our study first explored the link between CRC risk factors and CIMP-high CRC in an

doi:10.6342/NTU202300311

East Asian country. Our findings indicate that the association between CIMP-high CRC and some risk factors (age, sex, and BMI) may differ in East Asian and Western populations despite similar associated clinicopathological characteristics.

doi:10.6342/NTU202300311

Chapter III. The Study of TME in Metastatic *BRAF V600E* mutant CRC

3.1 Introduction

BRAF mutation is present in 4-8% of metastatic CRC, and *BRAF V600E* mutation is the most common variant of *BRAF* mutations[23,24]. Right-sided primary tumors, peritoneal and distant lymph node metastases, and *MLH1* hypermethylation are significantly associated with *BRAF* mutations in CRC, while *KRAS* mutation is mutually exclusive with *BRAF* mutations[22,77]. The consensus molecular subtypes (CMS) of CRC have recently been proposed based on pooled transcriptomic analyses[78]. There are four CMS subtypes (CMS 1-4); among them, CMS1 (MSI-Immune) tumors are characterized by more MSI-high, CIMP-high, *BRAF V600E* mutation, and infiltrative immune cells. *BRAF* mutations are also categorized into two *BRAF* mutant classifications (BM)[79]. Activation of the KRAS/AKT pathway, dysregulation of mTOR/4EBP, and epithelial-mesenchymal transition signaling occur in the BM1 subtype, and cell-cycle dysregulation is noted in the BM2 subtype. Kopetz et al. recently presented that 48.8%, 2.9%, 11.8%, and 36.5% of *BRAF V600E* mutant CRC corresponded to CMS1, CMS2 (canonical), CMS3 (metabolic), and CMS4

doi:10.6342/NTU202300311

(mesenchymal) subtype in the BEACON study[80]. They also showed that 33.1% and 66.9% of *BRAF V600E* mutant CRC belonged to BM1 and BM2 subtypes, respectively. In addition, CMS4 and BM1 subtypes were correlated with a higher objective response to cetuximab, encorafenib and binimetinib treatment. These findings revealed that there was heterogeneous gene expression in the TME of *BRAF V600E* mutant CRC, contributing to different efficacies of targeted therapy.

BRAF V600E mutation has been recognized as a poor prognostic factor in metastatic CRC, and patients with this genotype had approximately 11-14 months of OS, much shorter than the survival time in those with *RAS*/*BRAF* wild type and those with *RAS* mutations[18,81-83]. The mechanisms underlying the poor prognosis of *BRAF V600E* mutant CRC remain unknown. As mentioned in the earlier chapter, immune contexture in TME correlates with the clinical outcomes in patients with CRC. It is reasonable to hypothesize that the immune contexture may also have prognostic implications in patients with metastatic *BRAF V600E* mutant CRC. Currently, the transcriptomic data of *BRAF V600E* mutant CRC was mainly derived from early-stage tumors. Still, Mlecnik et al. showed the expression of immune-related genes in primary CRC tumors differed between metastatic and non-metastatic diseases. Thus, it is

doi:10.6342/NTU202300311

important to analyze the immune contexture in metastatic *BRAF V600E* mutant CRC.

The development of anti-PD-1/PD-L1 antibodies has changed the paradigms in many cancer types[84]. dMMR (or MSI-high) and high tumor mutational burden are the predictive biomarkers for anti-PD-1/PD-L1 antibodies[36,84,85]. According to previous studies, 42-48% of *BRAF V600E* mutant CRC belongs to CMS1 (Immune), which holds great potential for novel immunotherapy[78,80]. Indeed, clinical trials showed good responses in CRC concomitant with *BRAF V600E* mutation and MSI-high; however, for MSS *BRAF V600E* mutant CRC, anti-PD-1 monotherapy was ineffective, and the combination of targeted therapy and anti-PD-1 therapy is recently under investigation[86-89]. We further hypothesize that a novel treatment for metastatic MSS *BRAF V600E* mutant CRC can be developed after illustrating the prognostic roles of immune contexture of TME in these tumors. Thus, we designed this study to recruit patients with *de novo* Stage 4 MSS *BRAF V600E* mutant CRC and perform the transcriptomic analysis on their primary tumors.

3.2 Methods

Patient enrollment

doi:10.6342/NTU202300311

Patients who met the following inclusion criteria were eligible for this study: (1) they had pathologically confirmed *de novo* metastatic *BRAF V600E* mutated CRC, which referred to distant metastases at diagnosis; (2) they had colectomy for CRC; and (3) they had MSS CRC. Patients who received systemic chemotherapy or targeted therapy before colectomy were ineligible for this study. We enrolled patients from two medical centers: NTUH and Kaohsiung Chang Gung Memorial Hospital (KCGMH, Kaohsiung, Taiwan). At NTUH, we searched the medical records on the *BRAF* mutation examination from 2010 to 2017. The codes for *BRAF* mutation analyses included 000W0406 for expanded *RAS*+*BRAF* mutation, 000W0389 for *KRAS* and *BRAF* mutations, and 000W0404 for *BRAF* mutation alone. Then we could identify patients with *de novo* metastatic *BRAF V600E* mutated CRC. In addition, we included the patients who met the inclusion/exclusion criteria from our previous cohort (2005-2013). Finally, another cohort from KCGMH was also enrolled. We collected patients' clinicopathological characteristics, in terms of age, sex, histology, tumor grade, disease stage at diagnosis, primary tumor location, systemic chemotherapy, targeted therapy, and survival time from electronic medical records. Patients were recognized to have right-sided tumors if the primary tumors were located from the cecum to the splenic

doi:10.6342/NTU202300311

flexure of the transverse colon. Patients had left-sided tumors if the primary tumors were located from the descending colon to the rectum. The definition of first-line triplet chemotherapy was the anti-cancer therapy consisting of oxaliplatin, irinotecan, and one of the fluoropyrimidines. The first-line doublet referred to the anti-cancer therapy consisted of one of the fluoropyrimidines and either oxaliplatin or irinotecan. This study was approved by the Institute Review Board of NTUH and KCGMH.

***BRAF V600E* mutational analysis**

The methods for detecting *BRAF V600E* mutation at NTUH include PCR and direct sequencing (ABI 3730 sequencer (Applied Biosystems, Foster City, CA, USA). The primer pairs (5'-TCA TAATGCTTGCTCTGATAGGA-3' and 5' - GGCCA AAAATTTAATCAGTGGA-3') covering *BRAF* exon 15 were used. On the other hand, *BRAF V600E* mutation was identified by Roche *BRAF*/*NRAS* Mutation Test (Roche Diagnostics, IN, USA) at KCGMH following the manufacturer's instructions. We performed *BRAF* mutation subtype classification (BM1 and BM2) by linear regression classifier as described in a previous study[79].

MSI analysis

The method for MSI testing and the definitions of MSI-high and MSS have been

doi:10.6342/NTU202300311

described in chapter 2.

Transcriptomic analysis

We extracted total RNA from the FFPE samples of primary colon tumors derived from colectomy using Qiagen's miRNeasy FFPE Kit (Qiagen, Valencia, CA, USA). Macrodissection of tumor slides was performed before RNA extraction. Then we used NanoDrop 2000 at 220–320 nm (Thermo Scientific) to measure 260/280 ratios to determine RNA quality and quantity. Bioanalyzer (model 2100, Agilent Technologies, Santa Clara, CA, USA) was used to measure nucleic acid fragmentation. Finally, the gene expression was evaluated by nCounter PanCancer Immune Profiling Panel (NanoString, Seattle, WA, USA). This panel consists of 770 genes and is widely used to investigate TME. We processed raw data as previously described[90]. Gene counts for each sample were normalized first by trimmed mean of M-values method[91] and then converted to log2-transformed counts per million later for clinical analysis.

Development of complement scores

We calculated pairwise expression correlation in complement genes according to the similarity metric of Pearson's correlation coefficient[92]. The results were regarded as an input for hierarchical clustering. Then the complement genes were classified into

doi:10.6342/NTU202300311

three co-expression modules, and the clustering results were shown by a heatmap symmetrical along the diagonal line. The complement score of each sample was determined as the average gene expression in module 2. A high complement score was defined when the complement score was higher than the median score; in contrast, a low complement score was defined when the complement score was lower than the median score.

Evaluation of immune cell abundance

The immune cell abundance in the TME of each tumor was measured according to its expression profiles. The simple average of marker genes' expression values of each immune cell was calculated as cell-type scores. The reference marker genes were determined by Danaher et al.[93]. We also used the CIBERSORT algorithm with the LM22 signature matrix to measure cell abundance[94]. The phenotypes of macrophages (M1 and M2) were defined based on the mean expression values of gene signatures[95]. The genes correlated to M1 macrophage consist of *CD40*, *CD86*, *CCL5*, *CCR7*, *CXCL9*, *CXCL10*, *CXCL11*, *IL1A*, *IL1B*, *IL6*, *IRF1*, *IRF5, IDO1*, and *KYNU*, and the M2 macrophage-associated genes are *CD276*, *CCL4*, *CCL13*, *CCL18*, *CCL20*, *CCL22*,

doi:10.6342/NTU202300311

CTSA, *CTSB*, *CTSC*, *CTSD*, *CLEC7A*, *FN1*, *IL4R*, *IRF4*, *LYVE1*, *TGFB1*, *TGFB2*, *TGFB3*, *TNFSF8*, *TNFSF12*, *MMP9*, *MMP14*, *MMP19*, *MSR1*, *VEGFA*, *VEGFB,* and *VEGFC*.

External cohorts

The first external cohort was colon and rectal adenocarcinomas in the TCGA dataset[96]. Genomic and transcriptomic data of these tumors were obtained from Genomic Data Commons through the R package of TCGA bio-links, and these tumors' microsatellite status was obtained according to the method described preciously[97]. The second external cohort was GSE39582 dataset[98]. Complement scores of all these CRC tumors from two external cohorts were calculated, and tumors were determined to have high or low complement scores based on the abovementioned definitions.

Immunohistochemical staining

The collected FFPE tumor tissues were cut into 5-μm sections, and then these sections were deparaffinized by EZ prep (Ventana Medical Systems, Inc., Tucson, AZ, USA). These sections were also pretreated with Cell Condition 1 solution for 32 minutes (Ventana Medical Systems, Inc.). We incubated the slides with anti-human C4d (clone A24-T, DB Biotech) and used the automated Ventana Benchmark XT for 1:200

doi:10.6342/NTU202300311

titration (Ventana Medical Systems, Inc.). Labeling was measured using the Optiview DAB Detection Kit (Ventana Medical Systems, Inc.). All sections were counterstained with hematoxylin in Ventana reagent, and the positive controls were the human FFPE tonsil tissues.

C4d is generated after C4 splitting during the activation of the complement pathway. C4d is a surface-bound protein that binds to tissue near the activation site because its covalent bond does not break spontaneously[99]. Thus, C4d is recognized as a marker of complement activation. We categorized CRC into three groups based on the percentages of C4d deposits on the tumor cell membrane. C4d-IHC 0 (weak) referred to <1% of non-neoplastic cells, C4d-IHC 1 (intermediate) was defined as 1%–30% of non-neoplastic cells, and C4d-IHC 2 (high) was defined as >30% of non-neoplastic cells. Semi-quantification was evaluated by two independent pathologists.

Statistical analysis

Patients' clinical and pathological data were summarized as percentages. Survival analyses among groups, including PFS, OS, and progression-free interval (PFI), were evaluated using the Kaplan-Meier method. A *p*-value of less than 0.05 in the log-rank test was considered significant. We developed a Cox proportional hazards regression

doi:10.6342/NTU202300311

model for survival analysis with the coxph function implemented in the R package. PFS in this study was defined as the period from the date of diagnosis to the date of radiographically confirmed progression of disease or death during first-line therapy. OS in this study was defined as the time from diagnosis to death. PFI was specifically used in TCGA and GSE39582 datasets to evaluate clinical outcomes[96,98]. PFI was defined as the time from the date of diagnosis to the date of the first evidence of disease progression, locoregional recurrence, new primary tumor, distant metastasis, or death. Only variables with $p < 0.1$ were included in the multivariate analysis. We used Benjamini and Hochberg multiple-testing correction method to adjust multiple tests. The statistical analyses and visualization in this study were performed in an R environment (version 3.6.1).

3.3 Results

A total of 54 patients with *de novo* metastatic CRC with MSS *BRAF V600E* were included in this study, among whom 31 were enrolled from the National Taiwan University Hospital-integrated Medical Database (NTUH-iMD), five from our previous cohort[27], and 18 from KCGMH. The detailed consort diagram of the enrollment of patients is presented in Figure 2. The patient's clinicopathological features are presented

doi:10.6342/NTU202300311

in Table 8. Briefly, the median age of patients was 51 years old; among these patients, 79.6% had low-grade tumors, 63% had right-sided primary tumors, and 42% had peritoneal metastases. No patients had concomitant *BRAF* and *KRAS* mutations. Two patients did not receive anti-cancer therapy after surgery and thus were not included in the PFS analysis; their median PFS was 5.1 months, and their median OS was 16.8 months (Figure 3).

After profiling the transcriptome of all tumors, the association between immune cell subtypes and patient survivals revealed that CD4+ T cell and B cell signatures were significantly correlated with longer PFS (Hazard ratio, HR= 0. 61, p = 0.005 for CD4+ T cell and HR = 0.72, p = 0.039 for B cell), and no immune cell types were significantly associated with patient OS (Table 9). In the analyses of the association between immune gene expression and patient survival, we found some checkpoints responsible for linking B cell and T cell signaling, such as *ICOS* (inducible T cell costimulatory) (PFS, HR = 0.0.71, p = 0.035), *ICOSLG* (inducible T cell costimulatory ligand) (OS, HR = 0.69, p = 0.034) and *CD40LG* (CD40 ligand) (PFS, HR = 0.62, p = 0.010), were associated with longer survival time. In contrast, there was no association between CD40, CD80, or CD86 and prognosis (Table 10). Besides, there were prognostic

doi:10.6342/NTU202300311

implications in the expression of complement genes. The key findings include that tumors with higher expression of *CR1*, *CD59*, *C1QA*, and *MBL2* were significantly associated with shorter OS than those with lower expression of these genes. Tumors with higher expression of *C1S, C1R,* and *SERPING1* were significantly associated with shorter PFS than tumors with lower expression of them (Table 11). Thus, the complement pathway may predict patients' prognosis in those with *de novo* metastatic CRC with MSS and *BRAF V600E* mutation. We first assessed the expression correlation of complement genes because the complement system involves various genes and pathways and showed that they could be grouped into three co-expression modules (Figure 4A). Subsequently, we grouped the patients into two groups according to the clustering of genes in each module. Patients with high expression of complement genes (Cluster 2) (Figure 4B) in their tumors had significantly shorter PFS (p = 0.00066) and a trend for shorter OS (p = 0.087) when module 2 (most genes belong to the classical complement pathway) was used for stratification (Figure 4C). Module 1 and Module 3 did not have sufficiently clear gene data for stratification (Figure 5).

To develop a better prognostic panel, we generated a complement score, which was calculated by measuring the average gene expression value in module 2 (Figure 6A).

doi:10.6342/NTU202300311

We used the median value of complement scores as the threshold to determine tumors with low and high scores. The survival analyses showed that patients with a high complement score had significantly shorter PFS (p = 0.029) and OS (p = 0.007) than those with a low complement score (Figure 6B). Furthermore, this complement score did not correlate with specific metastatic sites (Figure 7). As expected, complement scores generated based on the genes in Modules 1 and 3 were not correlated with PFS and OS (Figure 8). In the multivariate analysis, after adjusting for multiple tests, a high complement score was associated with significantly shorter OS (HR: 2.44, 95% confidence interval (CI): 1.26–4.70, adjusted p = 0.008) (Table 12). To validate the results of our study, we searched for external CRC cohorts in open datasets; six patients with metastatic *BRAF V600E* mutant CRC were included in both GSE39582 and TCGA datasets. Thus, Stage 1-4 *BRAF V600E* mutant CRC (N= 49 in GSE39582 dataset and N= 55 in the TCGA dataset) were used as the alternatives. The results showed a significantly shorter PFI (p = 0.03) and a trend for shorter OS (p = 0.37) in patients with a high complement score than in those with a low complement score in the GSE39582 cohort (Figure 6C). In the TCGA colon and rectal adenocarcinoma cohort, patients with a high complement score correlated with a non-significant shorter OS time than those

doi:10.6342/NTU202300311

with a low complement score (p = 0.056), and there was no significant difference in PFI between these two groups (Figure 9A). On the other hand, the TCGA cohort included 31 Stage 4 CRC with genotypes of MSS and *BRAF* wild type. In these tumors, a high complement score was not associated with a poor prognosis (Figure 9B). The correlation between a complement score and BM1 or BM2 was also analyzed in the GSE39582 and TCGA datasets. The results revealed that the complement scores in BM1 CRC were significantly higher than that in BM2 CRC (Figure 6D, Figure 9C).

In immunohistochemical staining, the density of intra-tumoral C4d-expression cells was semi-quantified (N=53). One patient was excluded from the analysis because of no available tissue sections for C4d staining. C4d staining was categorized into three groups. C4d-IHC 0 referred to low expression, C4d-IHC 1 to intermediate expression, and C4d-IHC 2 to high expression (Figure 10A). We evaluated the association between complement signatures and C4d expression in our cohort and showed that the complement scores in tumors with high ($p = 9.6e^{-4}$) and intermediate ($p = 5.5e^{-4}$) expressions of C4d were significantly higher than the scores in tumors with low expression (Figure 10B).

Recently, many studies indicate that in situ C1q produced by TAMs may

doi:10.6342/NTU202300311

contribute to intra-tumoral complement pathway activation[92,93]. This study evaluated the correlation between tumor-infiltrating immune cells and a complement score[93,94]. We used two independent methods to estimate immune cell abundance, and the result showed that macrophage abundance was strongly associated with the complement score (Figure 11A). Next, we analyzed the association between a complement score and the M1 or M2 signature and demonstrated that only the signature of M2 TAM ($\rho = 0.78$, $p < 10e^{-16}$; Figure 11B) but not the signature of M1 TAM was strongly correlated to the complement score.

3.4 Discussion

The complement system plays a major role in innate immunity against pathogens and homeostasis in the body[92]. More than 50 plasma components of complement are produced mainly in the liver, and the complement receptors are expressed on the membrane of many cell types. Recently, many studies revealed that complement effectors could be generated intracellularly, locally activate the complement pathway, and have non-canonical function independent of plasma cascades[100,101]. The in situ complement activation in TME may have an important role in disease progression and metastasis[102-104]. For example, C3a and C5a, known as anaphylatoxins, profoundly

doi:10.6342/NTU202300311

influence the immune cells in the TME. They can suppress T cell-mediated immunity by recruiting myeloid-derived suppressor cells, increasing TAM density, and decreasing the infiltration of CD4+ T cells and neutrophils[105-107]. Several studies demonstrated the prognostic roles of intra-tumoral complement in cancer patients[108]; among them, C1s and C4d expression acts as a prognostic factor of lung cancer and clear cell renal cell carcinoma, respectively[109,110]. In our study, we showed that a high complement score predicted poor prognosis in *de novo* metastatic CRC with MSS and *BRAF V600E* mutation, and the prognostic association between a complement score and patient's survival was also observed in patients with *BRAF V600E* mutant CRC (stage 1-4) in two external cohorts. We stained C4d in tumors to validate complement activation in TME, and the results demonstrated that C4d density was significantly correlated with the complement score in this study. By contrast, the prognostic implication of complement activation was not seen in metastatic CRC with MSS and wild-type *BRAF V600E* mutation in the TCGA cohort. However, further study is warranted to validate this finding because of the relatively small sample size.

BRAF mutations are classified into BM1 and BM2 according to different gene expression patterns[79]. Barras's study showed complement activation in BM1 tumors,

doi:10.6342/NTU202300311

which is supported by our study. Besides, higher complement scores were observed in BM1 tumors than in BM2 ones, possibly due to the overlap of genes analyzed for generating complement scores and BM1.

Complement activation is associated with TAM. Bonavita et al. reported that epigenetic silencing of *PTX3*, which encodes pentraxin protein that regulates complement activation, could enhance CCL2 production, TAM infiltration, and complement activation in CRC[106]. Another study highlighted that C1q-producing TAM infiltrated in the TME of RCC had a positive association with a high expression of immune checkpoints, including PD-L1, PD-L2, PD1, and LAG-3, in an immunosuppressive microenvironment[111]. In our study, only M2 TAM was strongly associated with the complement score in the TME in metastatic CRC with MSS and *BRAF V600E* mutation; TAM polarization correlated with prognosis in CRC. Vayrynen et al. demonstrated that a high M1:M2 density ratio in stroma predicted better cancer-specific survival, and M2 density was correlated with worse cancer-specific survival[63]. Edin and colleagues also showed that increased infiltration of M1 TAM in the invasive front of tumors was associated with better survival in CRC patients[112]. Thus, a high infiltration of M2 TAM may contribute to the observation that a high complement score

doi:10.6342/NTU202300311

is an independent factor for shorter survival in our patients.

One of the aims of this study is to develop novel strategies for treating metastatic *BRAF V600E* mutant CRC based on transcriptomic analyses. Of course, our data still needs further validation, but we can propose some ideas that warrant further exploration. The first is the combination of a complement inhibitor (ideally, C3a or C5a blockade) with an anti-PD1 or anti-PD-L1 antibody. The underlying mechanism is that the local production of C3a and C5a may induce an immunosuppressive TME and promote metastasis[92]. Ajona et al. used the combination of a C5a inhibitor and an anti-PD-1 or anti-PD-L1 antibody in a synergic murine lung cancer model. They demonstrated that the treatment was effective and the efficacy associated with the reinvigoration of CD8 T cells[113]. The second strategy combines a CSF1R inhibitor and an anti-PD-1 or anti-PD-L1 antibody. The underlying mechanism may be that CSF1R signaling regulates the polarization of macrophages and promotes M2 phenotype [114]. Thus, inhibition of the CSF1R signaling may reverse M1/M2 ratio in metastatic *BRAF V600E* mutant CRC. In an early phase study, two patients with proficient mismatch-repair CRC were responsive to pembrolizumab (anti-PD-1 antibody) and AMG820 (CSF1R antibody); however, the *BRAF* mutational analysis is still unknown[115].

doi:10.6342/NTU202300311

There are several limitations to our study. The first is that we only collected the tumor tissues derived from colectomy for better analyzing the immune contexture in the TME, which may have led to selection bias. However, according to our data, the patient's clinicopathological features were consistent with the literature, and their PFS and OS were similar to the historical data[18,22,23]. The second limitation is the small sample size; however, our result seems reproducible with external cohorts.

doi:10.6342/NTU202300311

Chapter IV. Conclusions and Future Perspectives

4.1 Prognostics, Carcinogenesis, Epigenetics, and Microbiome

In the first study, we demonstrated that divergent clinicopathological characteristics and risk factors correlated with CIMP-high CRC in different age groups in Taiwan. Our study validates the high frequency of CIMP-high genotype in EOCRC in Taiwan and highlights that a BMI of ≥ 27.5 kg/m^2 may be associated with those early-onset hypermethylated tumors.

Based on the findings in this study, we will explore the etiology of the increased incidence of EOCRC in Taiwan and the high frequency of CIMP-high CRC in younger patients. The growing incidence of EOCRC in Taiwan and worldwide in recent years is noticeable and worrisome[116]. The estimated global incidence of EOCRC in 2030 is expected to increase by more than 140%[117]. According to the previous study, the etiology of about 80% of EOCRC may be environmental exposures with or without the presence of genetic variants predisposing to CRC[118]. Environmental exposures include obesity, Westernized diets, antibiotics, dysbiosis, and others. Gut microbiota, specifically *Fusobacterium nucleatum, Bacteroidetes,* enterotoxigenic *Bacteroides fragilis*, and *Firmicutes*, are enriched in CRC and are potentially involved in

doi:10.6342/NTU202300311

carcinogenesis[119-121]. For the gut microbiota enriched in EOCRC, Yang et al. analyzed fecal samples to show that *Flavonifractor* was a key bacterial species not enriched in LOCRC[122]. Because tumor cells may have causative interaction with the microbiome in TME, the analysis of gut microbiota and the associated metabolites from tumor tissues may yield novel insights into the carcinogenesis of CRC[123]. Thus, we have initiated a study to explore the specific tumor microbiota in EOCRC since 2022. In this study, we plan to use fresh tumor tissues from the Biobank at NTUH, including EOCRC and LOCRC, in the discovery set, using polyps and adenomas from patients without CRC as the control group. On the other hand, we will prospectively collect fresh tumor tissues at four institutes, including NTUH, National Taiwan University Cancer Center, KCGMH, and Far-Eastern Memorial Hospital, in the validation set. The microbiome will be analyzed by 16S ribosomal RNA sequencing, and the gut microbiome-associated metabolites will be measured by mass spectrometry. Then we may identify the specific tumor microbiomes for EOCRC, CIMP-high tumors in EOCRC, and patients with CRC and a high BMI. These results will provide a new understanding of the epidemiology and prevention of CRC.

4.2 Prognostics, TME, and Complement Activation

doi:10.6342/NTU202300311

In the second study, we conclude that in patients with metastatic *BRAF V600E* mutant CRC, intra-tumor complement activation is associated with significantly shorter survival. Intra-tumor complement activation is also strongly correlated to the M2 phenotype of TAM signature, which may contribute to the poor prognosis of those patients. Based on these results, we have new research objectives to identify clinical markers for metastatic *BRAF V600E*-mutated CRC, explore the role of complement activation in early-stage *BRAF V600E* mutant CRC, and develop the application of complement inhibitor in *BRAF V600E* mutant CRC.

A clinically useful biomarker is usually related to a simple test in a hospital-based laboratory. Our previous study showed a strong correlation between C4d staining and complement score[124]. Thus, C4d staining may be a good predictor for the prognosis of patients with metastatic *BRAF V600E*-mutated CRC. Besides, a prior report showed that BM1 was associated with a higher response rate of the triplet combination of cetuximab, encorafenib, and binimetinib, and the BM subtype was not associated with the response to cetuximab and encorafenib[80]. Because BM1 is also strongly correlated to the complement score, we hypothesize that C4d staining may predict the response to the triplet. On the other hand, C1q-producing macrophages may play a key role in

doi:10.6342/NTU202300311

initiating complement activation in TME, so we hypothesized that C1q staining might also predict the prognosis of the patients with metastatic *BRAF V600E* mutant CRC[111]. Therefore, our ongoing study is to explore the prognostic implications of C4d and C1q staining in *BRAF V600E* mutant CRC.

In chapter 3, the analyses of two external CRC cohorts support that complement activation may predict poor survival in patients with Stage 1-4 *BRAF* mutant CRC; however, those analyses were not conclusive because they were mixed with MSI-high, a potential confounding factor, and their sample sizes were small. We thus have initiated a prospective study to collect early-stage *BRAF* mutant CRC since 2022 by cooperating with investigators from four institutes. We will explore the role of intra-tumoral complement activation and the association between intra-tumoral and plasma complements in early-stage MSS *BRAF* mutant CRC.

The next future work is to develop novel therapeutic strategies for metastatic *BRAF* mutant CRC. As mentioned earlier, we proposed complement inhibitors with or without anti-PD-1 antibodies for metastatic CRC with MSS and *BRAF V600E* mutation. Many studies showed convertase-independent C3 or C5 cleavage by proteases (procathepsin L, plasmin, thrombin, etc.) in cancer models[102,125,126]. The cascades-independent release

doi:10.6342/NTU202300311

of C3a or C5a had protumor effects probably because they induced immune-suppressive responses, neo-angiogenesis, and direct influence on tumor cells[92]. Ajona et al. demonstrated that combined blockade of C5a and anti-PD-1 reduced tumor growth and metastasis in a lung cancer syngeneic mouse model[113]. Zha et al. also showed their anti-tumor activity increased after blocking C5aR1 signaling in a murine colon cancer model[127]. Multiple C3 and C5 inhibitors have been approved for paroxysmal nocturnal hemolysis with the reduction of hemolysis and a moderate (about 30%) infection rate[128]. C3a or C5a inhibitors do not block the complement downstream effectors and formation of the membrane attack complex; thus, they are probably more suitable drugs for further development in cancer treatment.

4.3 Prognostics: Open the Door to Future CRC Research

Prognosis predicts a patient's outcomes based on current information. Clinically, evaluating a patient's prognosis is important because it helps physicians to choose proper treatment strategies and communicate with patients and their families. For example, the prognosis of patients with Stage IV CRC is poor; its common treatment strategies are palliative targeted therapy and chemotherapy to prolong survival and maintain the quality of life. On the other hand, the prognosis of patients with Stage I-III

doi:10.6342/NTU202300311

CRC who receive colectomy is favorable; thus, curative surgery is generally recommended. Prognosis is one of the clinical presentations of cancer biology. Therefore, studying prognosis could be the beginning of cancer biology research. For example, more than 20 years ago, Gryfe et al. reported that MSI-high CRC was less likely to metastasize to lymph nodes and distant organs than MSS CRC, and patients with MSI-high CRC had a better prognosis[31]. In recent years, studies revealed that increased Th1 cells and cytotoxic T cell infiltration were observed in the TME of MSI-high CRC compared to that in the TME of MSS CRC, and active immune responses may be one of the mechanisms that contribute to a favorable prognosis[33,35]. However, some cases of early-stage MSI-high CRC still progress to metastatic disease, and the mechanism of their immune evasion is undefined. Thus, we have conducted an ongoing study to address this question.

Studying prognosis can also identify patients with unmet medical needs for developing novel anti-cancer therapy. *RAS* mutations are a poor prognostic factor for metastatic CRC, and RAS is always the target for new drug development. While RAS has been recognized as undruggable in the past 50 years, a new class of KRAS G12C inhibitors targeting the GDP of G12C, was reported in 2013[129]. Two new KRAS G12C

doi:10.6342/NTU202300311

inhibitors (sotorasib and adagrasib) demonstrated clinical efficacy in *KRAS G12C* mutant non-small cell lung cancer and colorectal cancer[130,131]. Patients with metastatic *BRAF V600E* mutant CRC have the worst survival outcomes; thus, many studies try to develop new therapeutics for them[89]. The combination of an anti-EGFR antibody with a BRAF inhibitor has recently demonstrated encouraging results, and this combination is now tested in the front-line setting with or without chemotherapy[89]. We identify that complement activation is a poor prognostic factor for metastatic *BRAF V600E* mutant CRC; thus, complements are reasonable targets for those patients[124]. The abovementioned breakthroughs may change patients' prognosis, which is another merit of studying prognosis.

In addition to developing new treatments for patients with poor prognosis, we can investigate the epidemiology and risk factors of those cancer types, which would be helpful for early diagnosis and prevention. Taking CIMP-high CRC as an example, CIMP-high CRC is significantly associated with high BMI in EOCRC in Taiwan[3]. Although the causal relationship between a high BMI and CIMP-high CRC is still undefined, a proper BMI should be maintained to prevent this type of cancer.

Therefore, studying prognosis can open the doors to cancer research, which is what

doi:10.6342/NTU202300311

I have learned in my Ph.D. journey.

doi:10.6342/NTU202300311

Chapter V. Figures

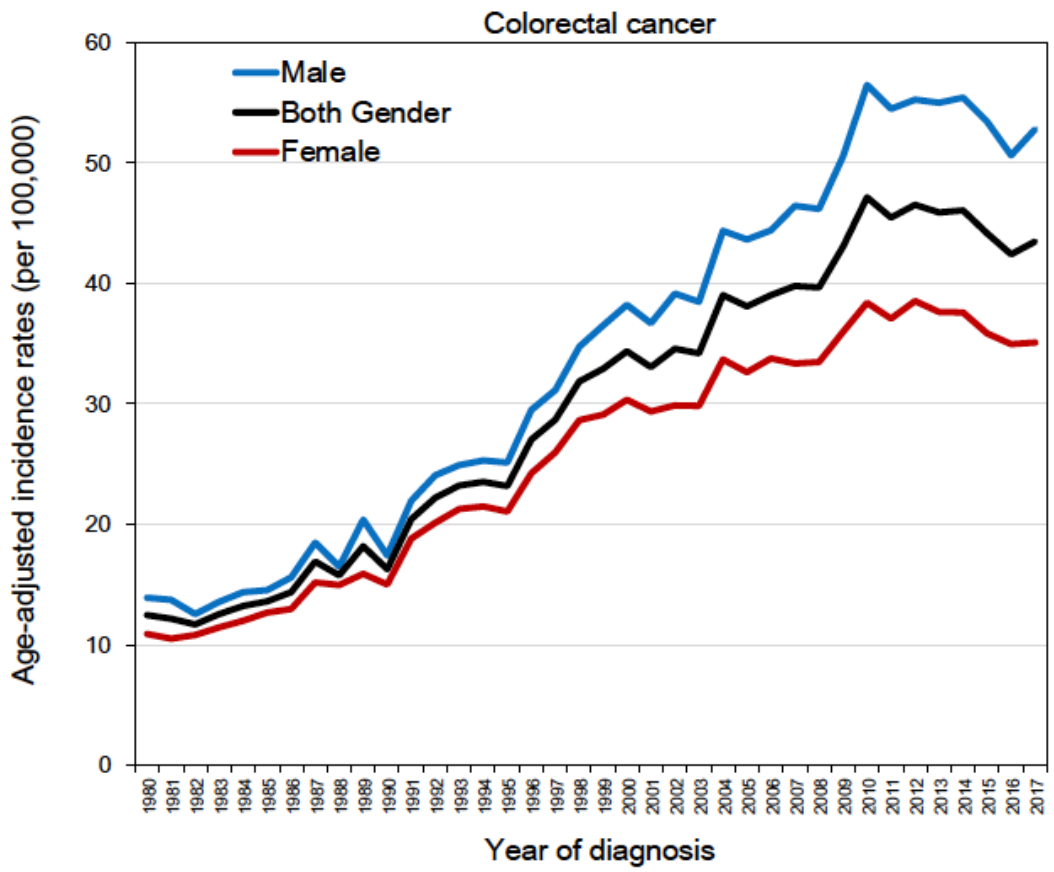

Figure 1. Age-adjusted incidence rates (ASR) of colorectal cancer (ICD 10 codes C18-C20) for both gender in Taiwan using the WHO standard population 2000. Data are obtained from Taiwan Cancer Registry Statistical Service (1980-2017)[3,132]. ICD10, International Classification of Disease 10th revision. WHO, World Health Organization.

doi:10.6342/NTU202300311

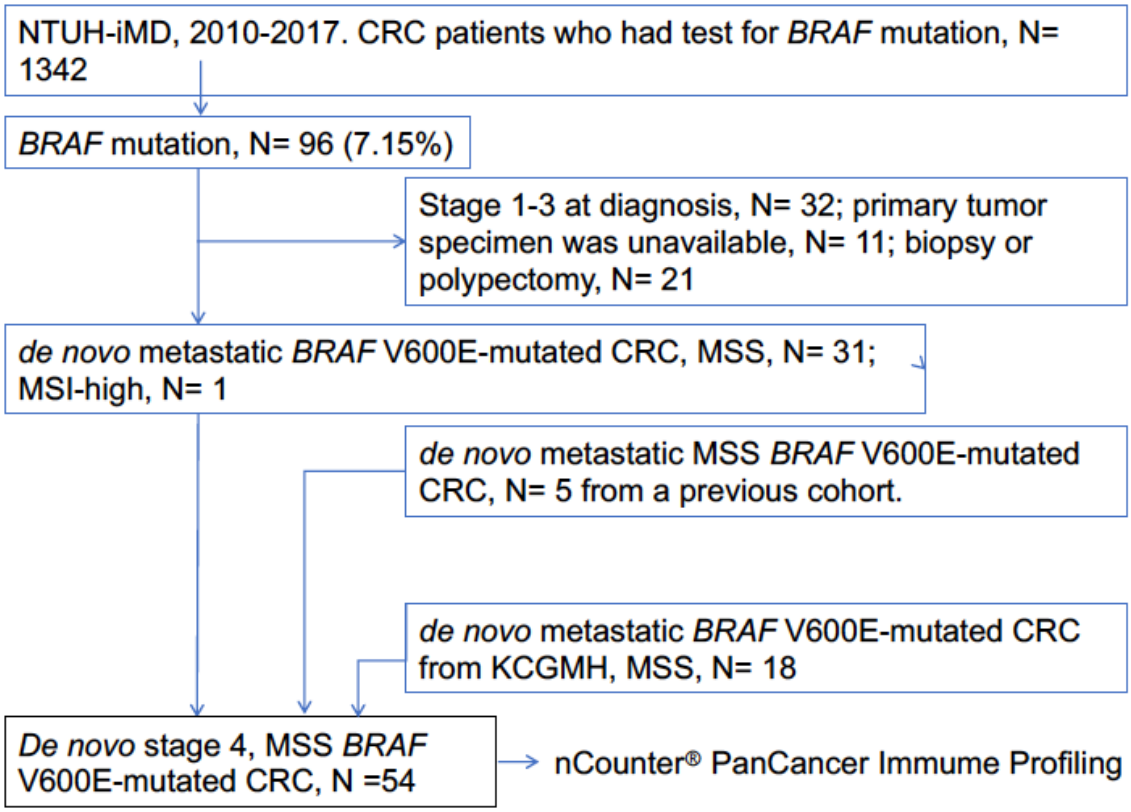

Figure 2. Flow chart of patient enrollment in this study[124]. CRC: colorectal cancer;

NTUH-iMD: Integrated Medical Database, National Taiwan University Hospital;

KCGH: KaoHsiung Chang Gung Memorial Hospital; MSI: microsatellite instability;

MSS: microsatellite stable.

doi:10.6342/NTU202300311

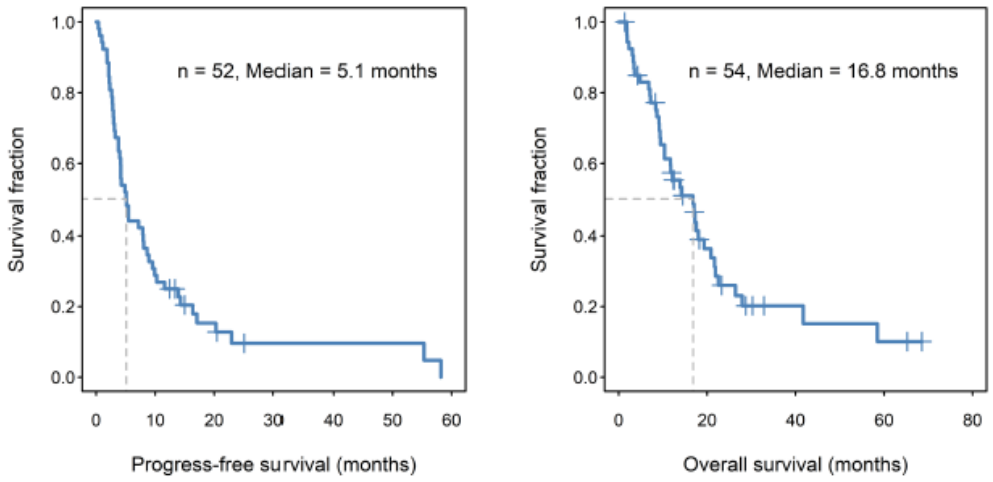

Figure 3. The survival probability in patients with *de novo* metastatic MSS *BRAF V600E* mutant CRC by Kaplan–Meier analysis[3]. *p*: log-rank test

doi:10.6342/NTU202300311

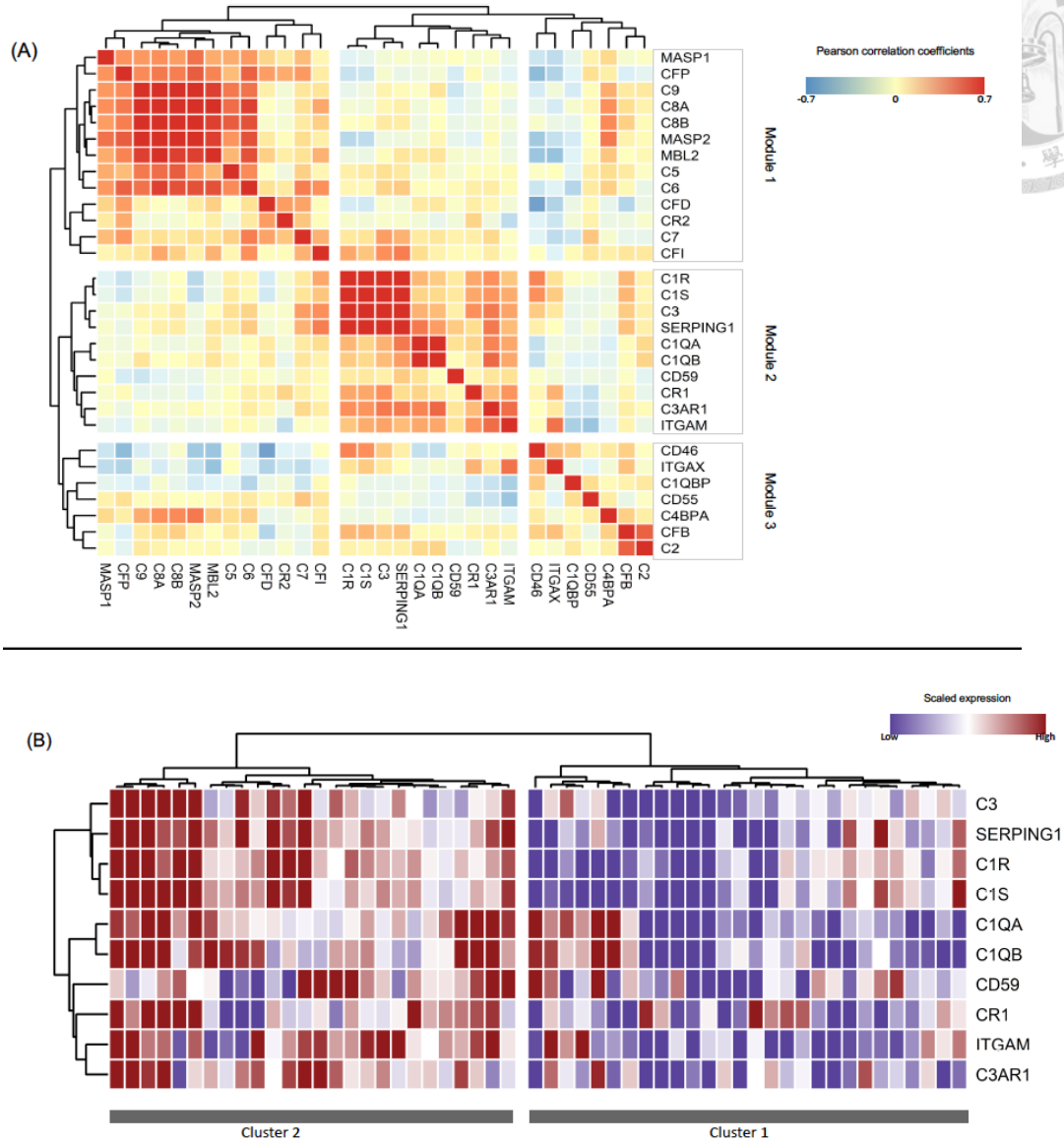

Figure 4. The prognostic implication of complement genes expression[124]. (A) Three co-expression modules of complement genes were identified. The expression correlations among genes were quantified by Pearson's correlation coefficient. (B) The two tumor clusters were based on the expression of complement genes in module 2.

doi:10.6342/NTU202300311

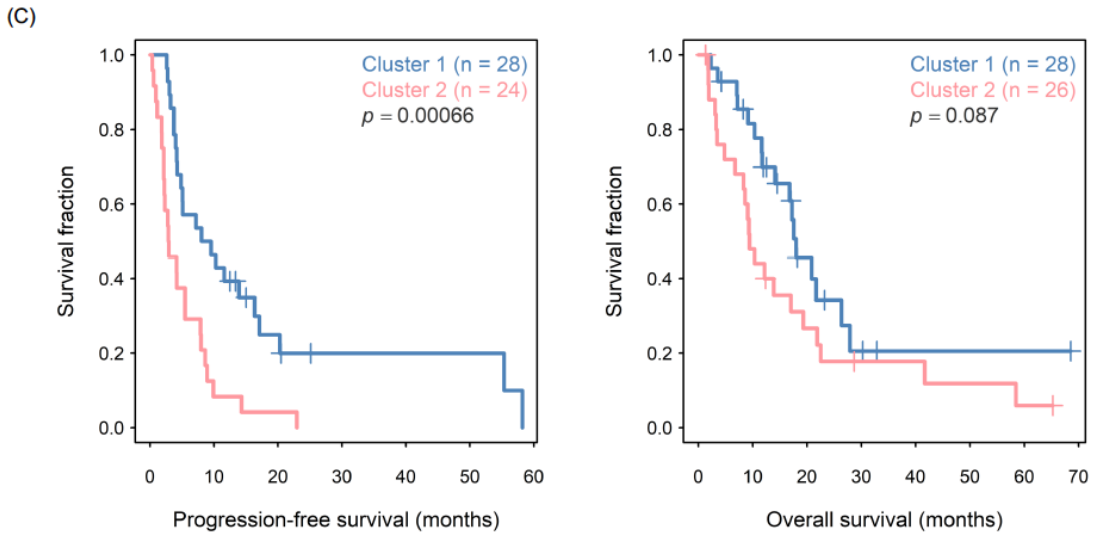

Figure 4. The prognostic implication of complement genes expression[124]. (C) The survival probability in patients with cluster 2 tumors compared with those with cluster 1 tumors by Kaplan–Meier analysis. *p*: log-rank test.

doi:10.6342/NTU202300311

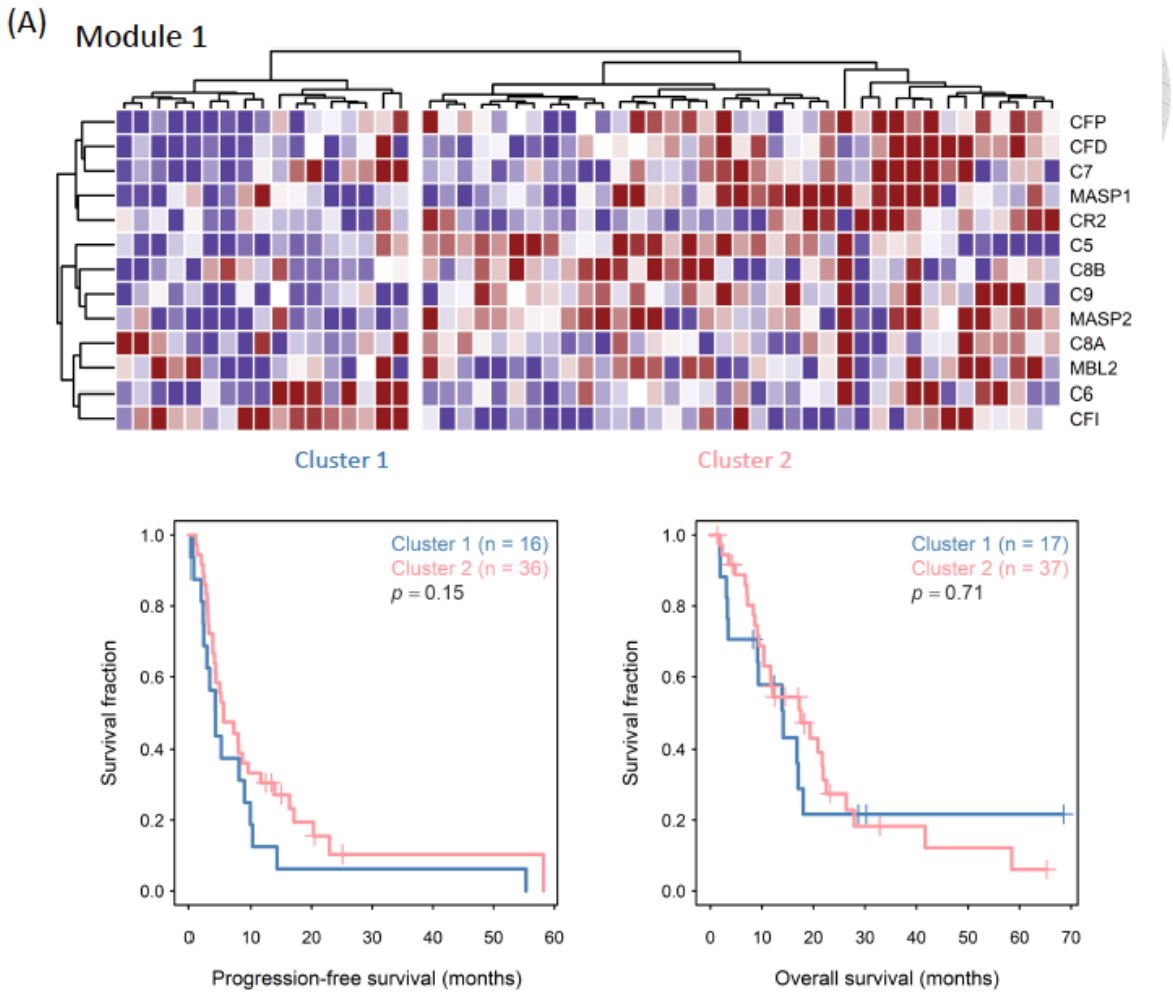

Figure 5. The prognostic implication of complement genes expression[124]. (A) Unsupervised hierarchical cluster analysis and the survival analysis by Kaplan–Meier method in patients defined by Module 1. *p*: log-rank test.

doi:10.6342/NTU202300311

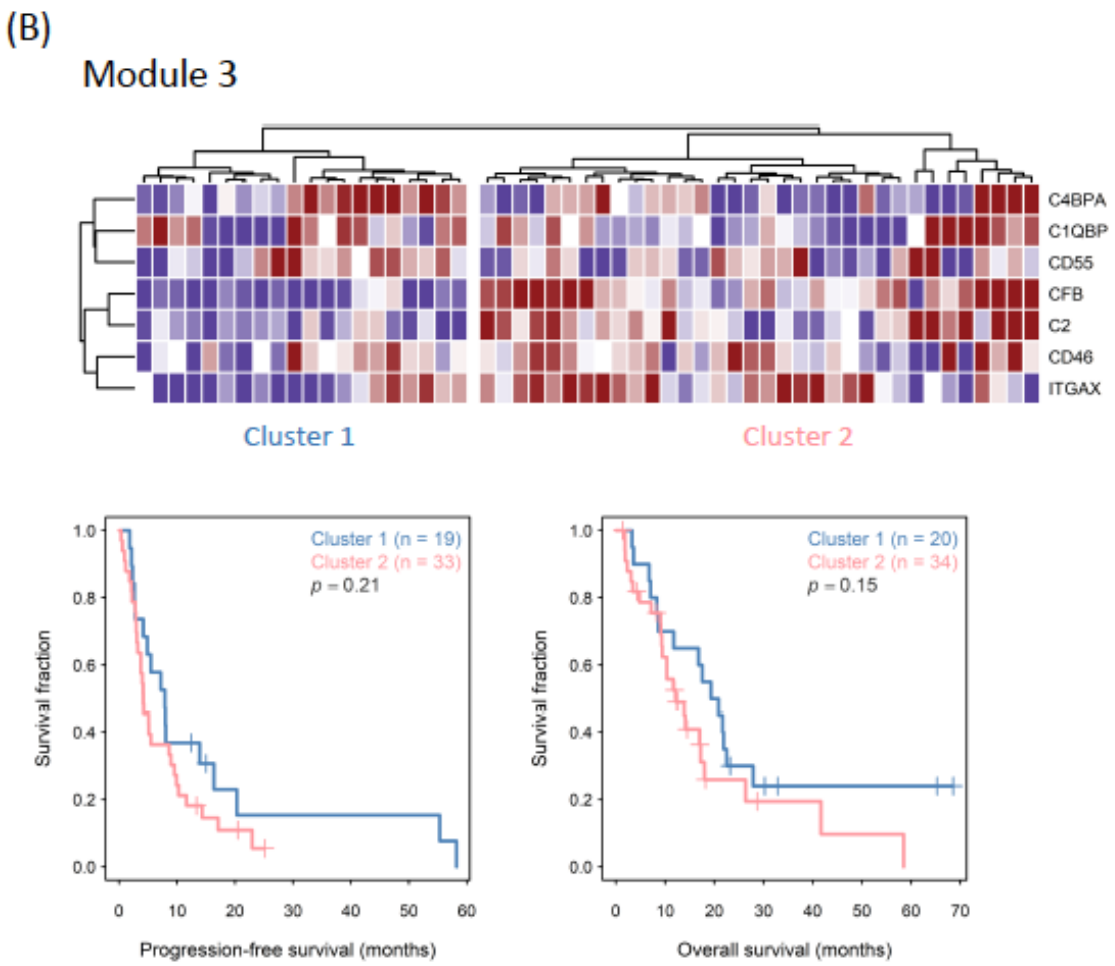

Figure 5. The prognostic implication of complement genes expression[124]. (B) Unsupervised hierarchical cluster analysis and the survival analysis by Kaplan–Meier method in patients defined by Module 3. *p*: log-rank test

doi:10.6342/NTU202300311

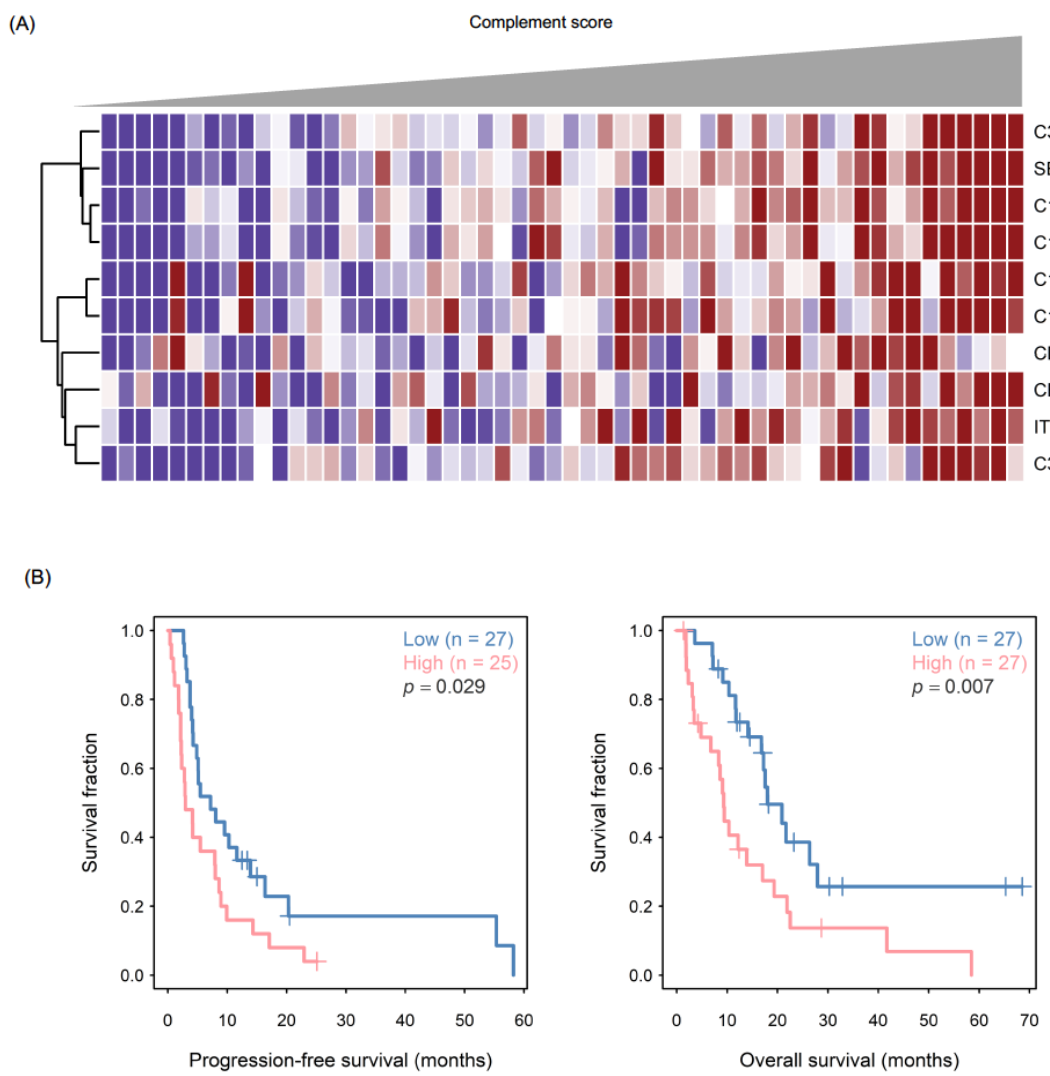

Figure 6. The prognostic values of complement score[124]. (A). The complement score was determined as the average expression of complement genes in module 2. (B). The survival probability by Kaplan–Meier analysis in patients with a high complement score compared with those with a low complement score in *de novo* metastatic MSS *BRAF V600E* mutant CRC in our cohort.

doi:10.6342/NTU202300311

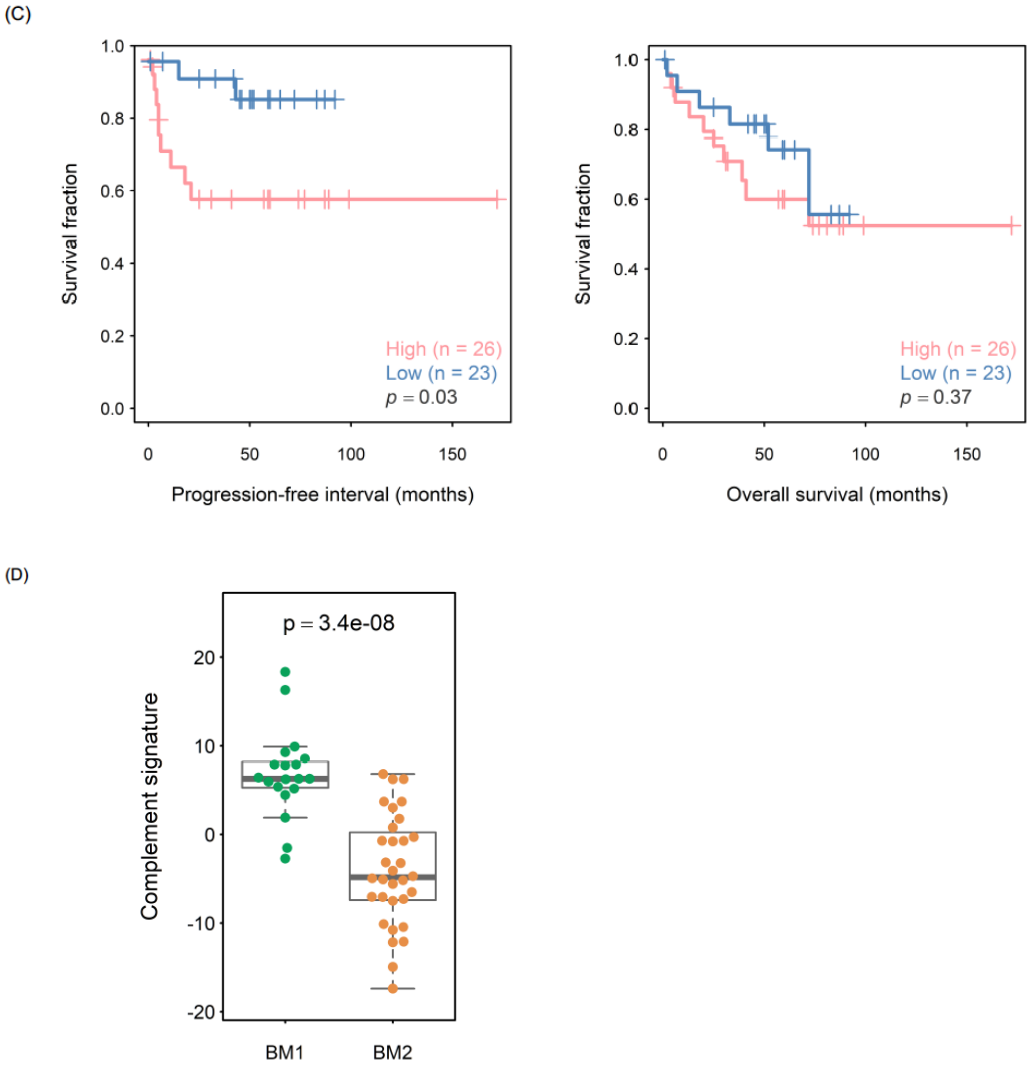

Figure 6. The prognostic values of complement score[124]. (C). The survival probability by Kaplan–Meier analysis in patients with a high complement score compared with those with a low complement score in *de novo* metastatic MSS *BRAF V600E* mutant CRC in stage 1-4 *BRAF V600E* mutant CRC in GSE39582 dataset. *p*: log-rank test. (D). The correlation of complement score and *BRAF* mutant (BM) classification in GSE39582 dataset. *p*: Wilcoxon signed-rank test.

doi:10.6342/NTU202300311

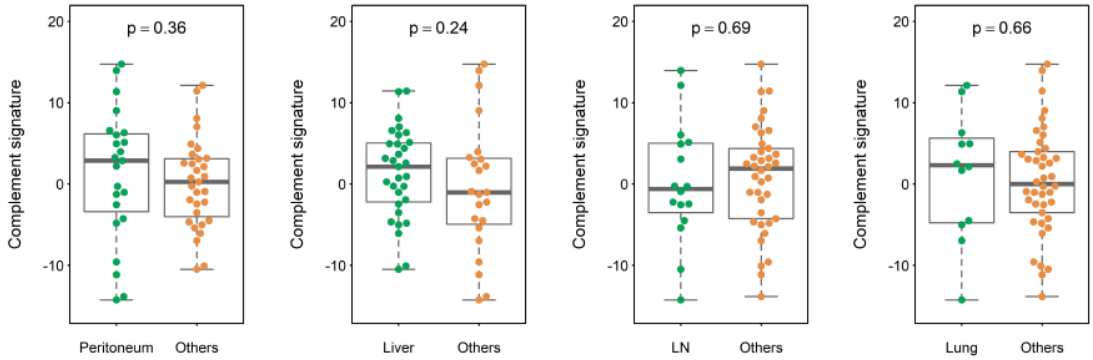

Figure 7. The correlation between complement score and the specific metastatic sites. *p*: Wilcoxon signed-rank test[124].

doi:10.6342/NTU202300311

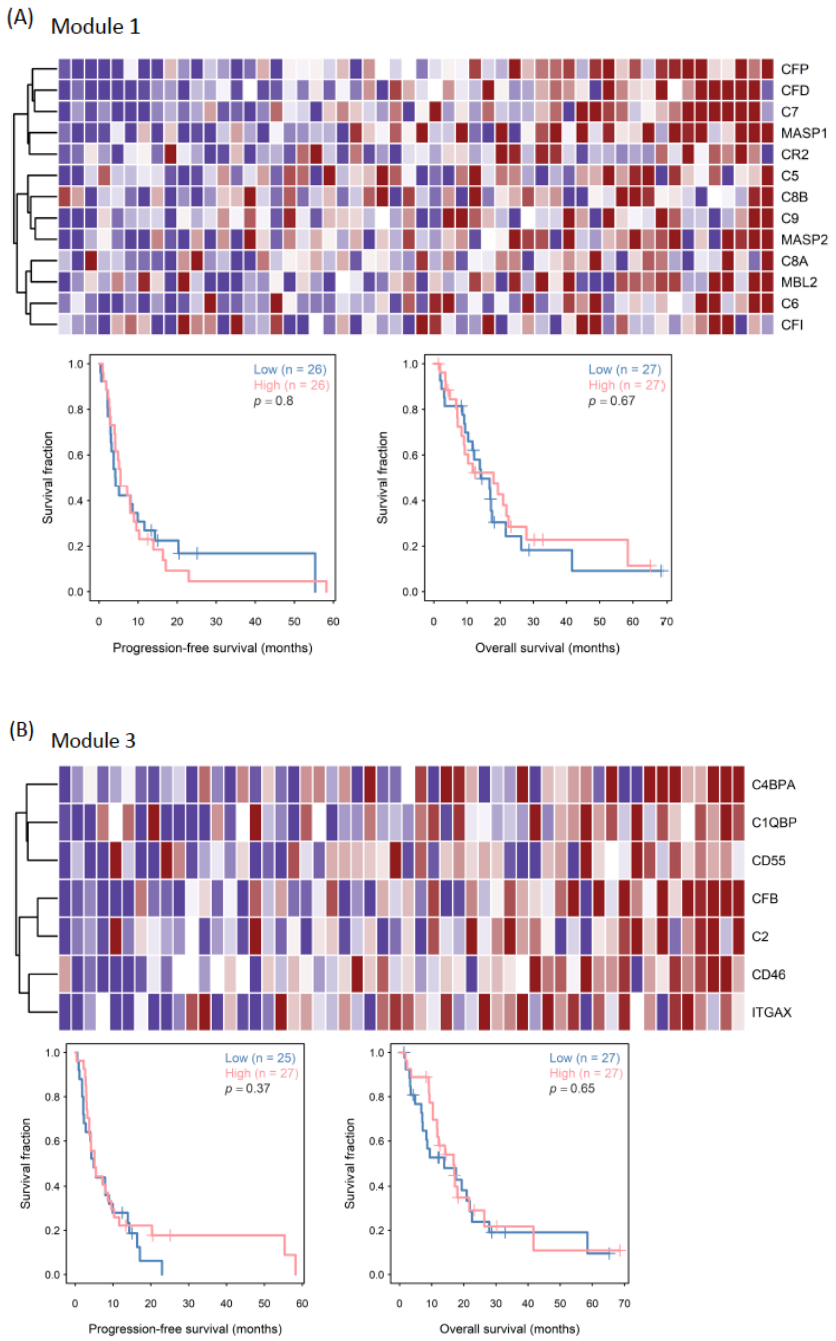

Figure 8. The survival probability by Kaplan–Meier analysis in patients with low and high complement scores defined by (A)Module 1 and by (B) Module 3[124]. *p*: log-rank test

doi:10.6342/NTU202300311

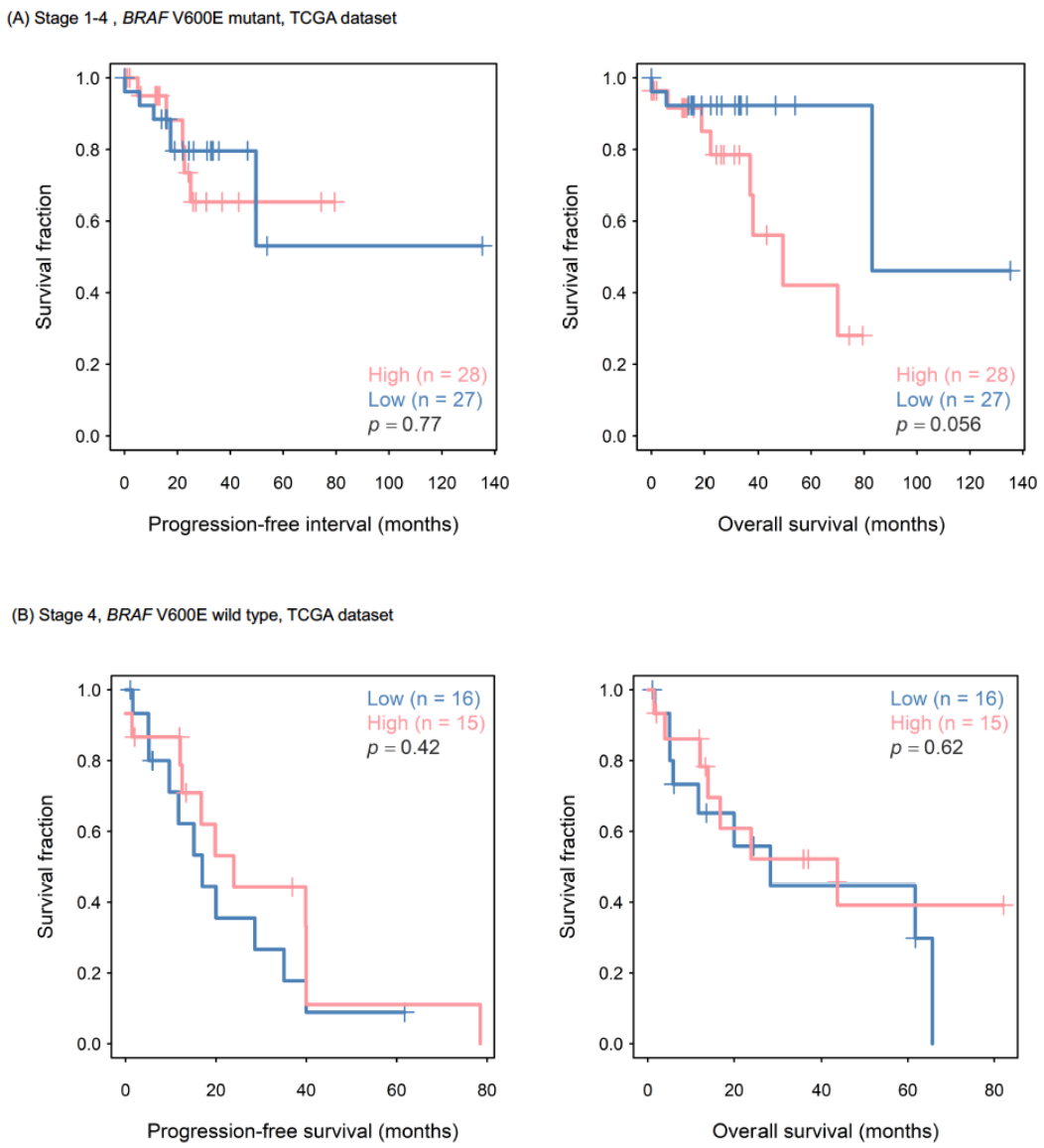

Figure 9. The survival probability by Kaplan–Meier analysis in patients with a high complement score compared with those with a low complement score in (A) stage 1-4 *BRAF V600E* mutant CRC and (B) stage 4 MSS *BRAF V600E* wild-type CRC in TCGA dataset[124]. *p*: log-rank test.

doi:10.6342/NTU202300311

(C) Stage 1-4 , *BRAF* V600E mutant, TCGA dataset

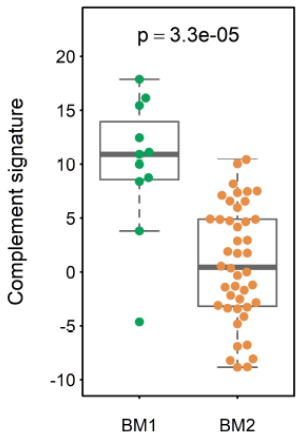

Figure 9. (C) The correlation of complement score and *BRAF* mutant classification in TCGA dataset[124]. *p*: Wilcoxon signed-rank test.

doi:10.6342/NTU202300311

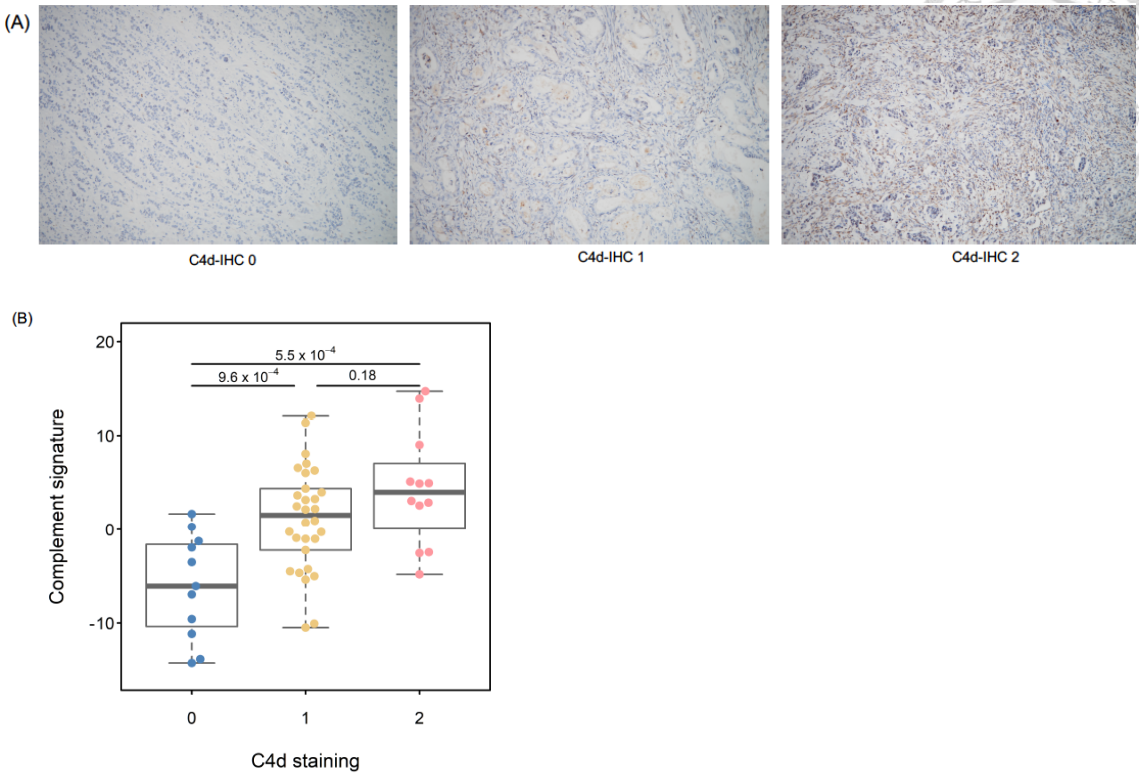

Figure 10. The correlation of the complement score and C4d density in *de novo* metastatic MSS *BRAF V600E* mutant CRC[124]. (A) Representative IHC staining for C4d on FFPE CRC tumor sections (100×). C4d-IHC 0 (low expression): cutoff of <1% of non-neoplastic cells; C4d-IHC 1 (intermediate expression): 1%–30% of non-neoplastic cells; C4d-IHC 2 (high expression): >30% of non-neoplastic cells. (B). The correlation between C4d density and the complement score. *p*: Wilcoxon signed-rank test.

doi:10.6342/NTU202300311

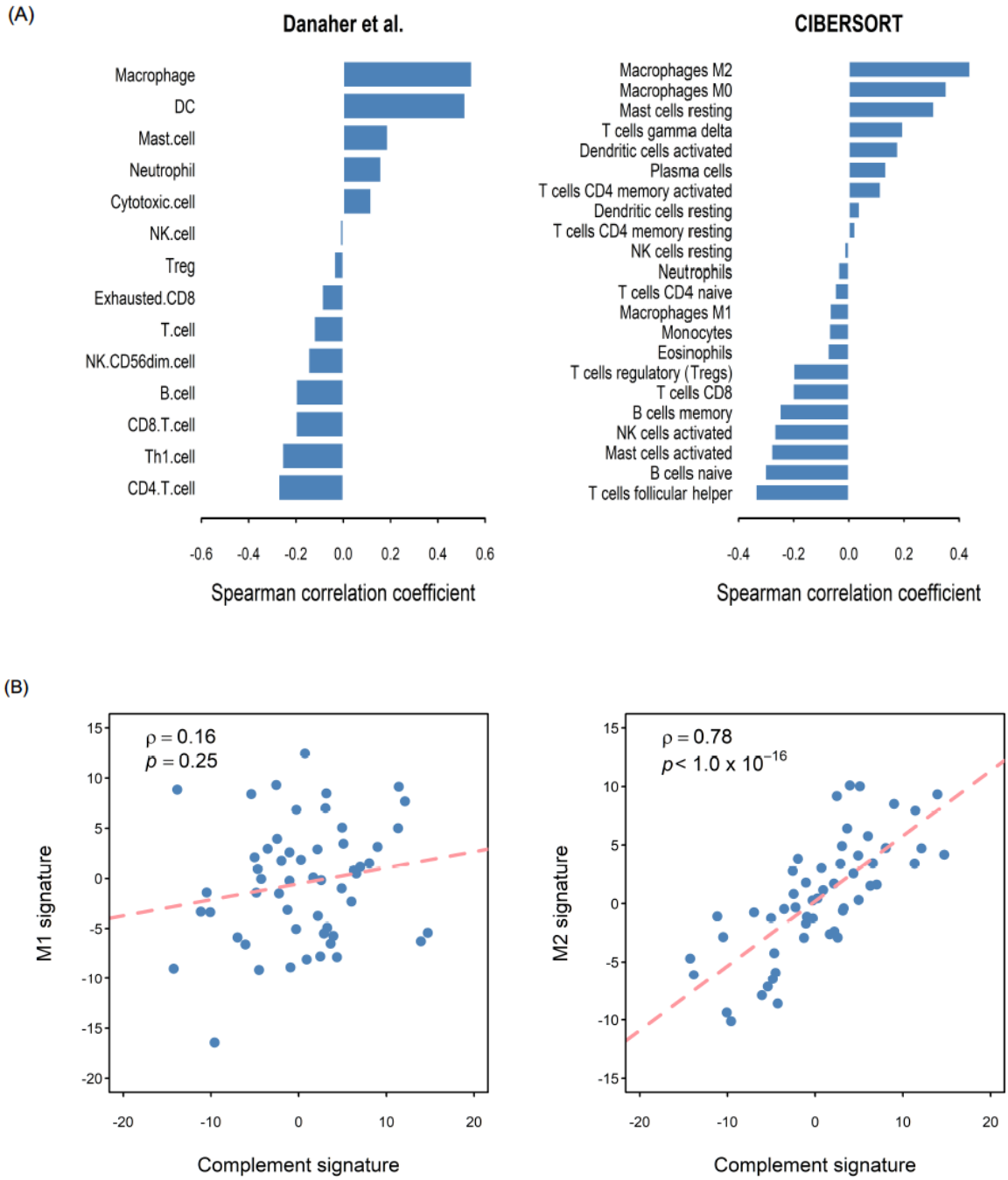

Figure 11. The analysis of immune cell abundance revealed a strong association between the complement score and M2 macrophages[124]. (A) The associations between the complement score and tumor-infiltrative leukocytes. Two independent methods were used for this analysis. (B). The complement score was strongly correlated to the M2 signature but not with the M1 signature. *r*: Spearman correlation coefficient.

doi:10.6342/NTU202300311

Chapter VI. Tables

Table 1. The primers used for CpG Island Methylator Phenotype testing in MethyLight study[3].

Primers	Sequence (5′ to 3′)
ALU-rtF *ALU*-rtR *ALU* probe	GGTTAGGTATAGTGGTTTATATTTGTAATTTTAGTA ATTAACTAAACTAATCTTAAACTCCTAACCTCA 6FAM-CCTACCTTAACCTCCC-MGBNFQ
p16-rtF *p16*-rtR *p16* probe	TGGAGTTTTCGGTTGATTGGTT AACAACGCCCGCACCTCCT 6FAM-ACCCGACCCCGAACCGCG-MGBNFQ
h*MLH1*-rtF h*MLH1*-rtR h*MLH1* probe	AGGAAGAGCGGATAGCGATTT TCTTCGTCCCTCCCTAAAACG 6FAM-CCCGCTACCTAAAAAAATATACGCTTACGCG-MGBNFQ
MINT1- rtF *MINT1*- rtR *MINT1* probe	GGGTTGAGGTTTTTTGTTAGCG CCCCTCTAAACTTCACAACCTCG 6FAM-CTACTTCGCCTAACCTAACGCACAACAAACG-MGBNFQ
MINT2- rtF *MINT2*- rtR *MINT2* probe	TTGAGTGGCGCGTTTCGT TCCCCGCCTAAACCAACC 6FAM-CTTACGCCACCGCCTCCGA-MGBNFQ
MINT31- rtF *MINT31*- rtR *MINT31* probe	GTCGTCGGCGTTATTTTAGAAAGTT CACCGACGCCCAACACA 6FAM-ACGCTCCGCTCCCGAATACCCA-MGBNFQ

doi:10.6342/NTU202300311

Table 2. Distribution of CIMP-high or CIMP-low/negative according to clinicopathologic variables. Logistic regression was used for statistical analysis[3].

Variable, N (%)	CIMP-high CRC (N = 45)	CIMP-low/negative CRC (N = 248)	OR (95% CI) high vs. low/negative	*p*-value
Age (years)				
< 50	14 (31.1)	75 (30.2)	reference	
≥ 50	31 (68.9)	173 (69.8)	0.96 (0.48-1.91)	0.91
Sex				
Male	22 (48.9)	135 (54.4)	reference	
Female	23 (51.1)	113 (45.6)	1.25 (0.66-2.36)	0.49
Stage†				
1	7 (15.6)	41 (16.5)	reference	
2	8 (17.8)	72 (29.0)	0.65 (0.22-1.93)	0.44
3	17 (37.8)	96 (37.1)	1.08 (0.42-2.81)	0.87
4	13 (28.9)	39 (17.3)	1.77 (0.64-4.88)	0.27
Histology				
Mucinous adenocarcinoma	3 (6.8)	8 (3.2)	reference	
Not mucinous adenocarcinoma	42 (93.3)	240 (96.8)	0.41 (0.10-1.64)	0.21
Tumor grade				
Low	39 (86.7)	230 (92.7)	reference	
High	5 (11.1)	13 (5.2)	2.27 (0.77-6.72)	0.14
Missing	1 (2.2)	5 (2.0)	NA	
Primary tumor side††				
Left-sided	18 (40.0)	126 (50.8)	reference	
Rectum	5 (11.1)	51 (20.6)	0.69 (0.24-1.95)	0.48
Right-sided	22 (48.9)	71 (28.6)	2.17 (1.09-4.31)	**0.03**
RAS				
Wild type	28 (62.2)	158 (63.7)	reference	
KRAS Mutation	16 (35.5)	83 (33.5)	1.09 (0.56-2.12)	0.81
NRAS Mutation	1 (2.2)	2 (0.8)	2.82 (0.25-32.17)	0.40

doi:10.6342/NTU202300311

Missing	0 (0.0)	5 (2.0)	NA	
BRAF V600E				
Wild type	26 (57.8)	238 (96.0)	reference	
Mutation	18 (40.0)	4 (1.6)	41.19 (12.96-130.95)	**< 0.01**
Missing	1 (2.2)	6 (2.4)	NA	
MSI				
Low/stable	31 (68.9)	229 (93.1)	reference	
High	14 (31.1)	17 (6.9)	6.08 (2.73-13.55)	**< 0.01**
Missing	0 (0.0)	2 (0.8)	NA	

Abbreviations: CIMP, CpG island methylator phenotype; OR, odds ratio; CI, confidence interval; MSI, microsatellite instability

† By the American Joint Cancer Committee on Cancer (AJCC) system, 7th edition.

†† The right-sided colon is defined as the cecum to the splenic flexure of the colon. The left-sided colon is defined as the region from the descending colon to sigmoid colon.

doi:10.6342/NTU202300311

Table 3. Distribution of CIMP-high or CIMP-low/negative according to clinicopathologic variables stratified by age. Chi-square test, and Fisher's exact test were used for statistical analysis[3].

	Age<50			Age≧50		
Variable, N (%)	CIMP-high CRC (N =14)	CIMP-low/negative CRC (N = 75)	*p*-value	CIMP-high CRC (N = 31)	CIMP-low/negative CRC (N =173)	*p*-value
Sex						
Male	8 (57.1)	47 (62.7)		14 (45.2)	88 (50.9)	
Female	6 (42.9)	28 (37.3)	0.70	17 (54.8)	85 (49.1)	0.56
Stage†						
1-3	5 (35.7)	59 (74.7)		27 (87.1)	149 (86.1)	
4	9 (64.3)	16 (25.3)	**< 0.01**[F]	4 (12.9)	24 (13.9)	1.00[F]
Histology						
Mucinous adenocarcinoma	1 (7.1)	2 (2.7)		2 (6.5)	5 (2.9)	
Not Mucinous adenocarcinoma	13 (92.9)	73 (97.3)	0.41[F]	29 (93.6)	167 (97.1)	0.29[F]
Tumor grade						
Low	11 (78.6)	69 (92.0)		28 (90.3)	161 (93.1)	
High	2 (14.3)	4 (5.3)	0.22[F]	3 (9.7)	9 (5.2)	0.40[F]
Missing	1 (7.1)	2 (2.7)		0 (0.0)	3 (1.7)	
Primary tumor side††						
Left-sided + rectum	9 (64.3)	60 (80.0)		14 (45.2)	117 (67.6)	
Right-sided	5 (35.7)	15 (20.0)	0.29[F]	17 (54.8)	56 (32.4)	**0.02**

doi:10.6342/NTU202300311

RAS							
	Wild type	9 (64.3)	50 (66.7)		19 (61.3)	108 (62.4)	
	Mutation	5 (35.7)	23 (30.7)	0.76 [F]	12 (38.7)	62 (35.8)	0.81
	Missing	0 (0.0)	2 (2.7)		0 (0.0)	3 (1.7)	
BRAF V600E							
	Wild type	8 (57.1)	71 (94.7)		18 (58.1)	167 (96.5)	
	Mutation	6 (42.9)	2 (2.7)	**<0.01** [F]	12 (38.7)	2 (1.2)	**<0.01** [F]
	Missing	0 (0.0)	2 (2.7)		0 (0.0)	3 (1.7)	
MSI							
	Low/stable	11 (78.6)	69 (92.0)		20 (64.5)	160 (93.6)	
	High	3 (21.4)	6 (8.0)	0.15[F]	11 (35.5)	11 (6.4)	**<0.01** [F]
	Missing	0 (0.0)	0 (0.0)		0 (0.0)	2 (1.2)	

Abbreviations: CIMP, CpG island methylator phenotype; OR, odds ratio; CI, confidence interval; MSI, microsatellite instability.

[F]Fisher's exact test

doi:10.6342/NTU202300311

Table 4. Distribution of CIMP-high or CIMP-low/negative according to risk factors of CRC in overall patients and stratified by age. Logistic regression was used for statistical analysis[3].

Variable, N (%)	Overall				Age<50				Age≧50			
	CIMP-high CRC (N =45)	CIMP-low/negative CRC (N =248)	OR (95% CI) high vs. low/negative	*p*-value	CIMP-high CRC (N =14)	CIMP-low/negative CRC (N =75)	OR (95% CI) high vs. low/negative	*p*-value	CIMP-high CRC (N = 31)	CIMP-low/negative CRC (N = 173)	OR (95% CI) high vs. low/negative	*p*-value
Family history												
None	42 (93.3)	218 (87.9)	reference		13 (92.9)	68 (90.7)	reference		29 (93.55)	150 (86.7)	reference	
Yes	3 (6.7)	30 (12.1)	0.52 (0.15-1.78)	0.30	1 (7.1)	7 (9.3)	0.75 (0.09-6.60)	0.79	2 (6.45)	23 (13.3)	0.45 (0.10-2.01)	0.30
Colorectal polyp												
0	32 (71.1)	209 (85.3)	reference		12 (85.7)	70 (93.3)	reference		20 (64.5)	139 (81.8)	reference	
≥ 1	13 (28.9)	36 (14.7)	2.36 (1.13-4.92)	**0.02**	2 (14.3)	5 (6.7)	2.33 (0.41-13.43)	0.34	11 (35.5)	31 (18.2)	2.47 (1.07-5.67)	**0.03**
BMI at diagnosis (kg/m^2), WHO criteria												
< 25	29 (64.4)	162 (65.7)	reference		7 (50.0)	51 (68.0)	reference		22 (71.0)	112 (64.7)	reference	
25-29	14 (31.1)	70 (28.2)	1.12 (0.56-2.26)	**0.74**	6 (42.9)	18 (24.0)	2.43 (0.72-8.19)	0.15	8 (25.8)	52 (30.1)	0.78 (0.33-1.88)	**0.58**
≥ 30	2 (4.4)	15 (6.1)	0.75 (0.16-3.45)	**0.71**	1 (7.1)	6 (8.0)	1.21 (0.13-11.63)	0.87	1 (3.2)	9 (5.2)	0.57 (0.07-4.69)	**0.60**

doi:10.6342/NTU202300311

BMI at diagnosis (kg/m^2)												
< 27.5	37 (82.2)	205 (82.7)	reference		9 (64.3)	63 (84.0)	reference		28 (90.3)	142 (82.1)	reference	
≥ 27.5	8 (17.8)	43 (17.3)	1.03 (0.45-2.37)	0.94	5 (35.7)	12 (16.0)	2.92 (0.83-10.24)	0.09	3 (9.7)	31 (17.9	0.49 (0.14-1.72)	0.27
DM												
None	37 (82.2)	201 (81.4)	reference		14 (100.0)	72 (96.0)	reference		23 (74.2)	129 (75.0)	reference	
Yes	8 (17.8)	46 (18.6)	0.95 (0.41-2.16)	0.89	0 (0.0)	3 (4.0)	NA	0.98	8 (25.8)	43 (25.0)	1.04 (0.43-2.51)	0.92
Hyperlipidemia												
None	31 (68.9)	189 (76.2)	reference		13 (92.9)	64 (85.3)	reference		18 (58.1)	125 (72.25)	reference	
Yes	14 (31.1)	59 (23.8)	1.45 (0.72-2.90)	0.30	1 (7.1)	11 (14.7)	0.45 (0.05-3.77)	0.46	13 (41.9)	48 (27.75)	1.88 (0.86-4.13)	0.12
NSAIDs use												
None	41 (91.1)	234 (94.7)	reference		13 (92.9)	75 (100.0)	reference		28 (90.3)	159 (92.4)	reference	
Yes	4 (8.9)	13 (5.3)	1.76 (0.55-5.65)	0.35	1 (7.1)	0 (0.0)	NA	0.99	3 (9.7)	13 (7.6)	1.31 (0.35-4.90)	0.69
HRT												
None	45 (100.0)	243 (98.4)	reference		14 (100.0)	75 (100.0)	reference		31 (100.0)	168 (97.7)	reference	
Yes	0 (0.0)	4 (1.6)	NA	NA	0 (0.0)	0 (0.0)	NA	NA	0 (0.0)	4 (2.3)	NA	0.98

Abbreviations: CIMP, CpG island methylator phenotype; OR, odds ratio; CI, confidence interval; BMI, body mass index; DM, diabetes mellitus; NSAIDs, non-steroidal anti-inflammatory drugs; HRT, hormone replacement therapy; WHO, world health organization.

doi:10.6342/NTU202300311

Table 5. Multivariate analysis for the association between CIMP-high CRC and clinicopathological variables in overall patients, patients with age < 50y and age ≥ 50y[3].

	Overall		Age < 50y		Age ≥ 50y	
Variable, N (%)	OR (95% CI) high vs. low/negative	*p*-value	OR (95% CI) high vs. low/negative	*p*-value	OR (95% CI) high vs. low/negative	*p*-value
Primary tumor site as right-sided	1.55 (0.67-3.60)	0.30			1.62 (0.69-3.82)	0.27
MSI-high	5.64 (2.06-15.45)	**<0.01**			5.86 (2.07-16.60)	**<0.01**
Colorectal polyp	1.33 (0.49-3.61)	0.58			1.38 (0.54-3.58)	0.50
BRAF V600E	38.86 (11.60-130.12)	**<0.01**				
Stage IV at diagnosis			10.021 (2.430-41.326)	**<0.01**		
BMI (≥ 27.5 kg/m^2)			5.657 (1.211-26.418)	**0.03**		

BRAF V600E mutation was excluded in multivariate logistic regression in patients with age <50y and age ≥ 50y because of few events were noted.

Abbreviations: CIMP, CpG island methylator phenotype; OR, odds ratio; CI, confidence interval; BMI, body mass index.

doi:10.6342/NTU202300311

Table 6. Distribution of CIMP-high or CIMP-low/negative according to clinicopathologic variables stratified by gender. Chi-square test, and Fisher's exact test were used for statistical analysis[3].

Variable, N (%)	Male			Female		
	CIMP-high CRC (N =22)	CIMP-low/negative CRC (N = 135)	*p*-value	CIMP-high CRC (N = 23)	CIMP-low/negative CRC (N =113)	*p*-value
Age						
<50	8 (36.4)	47 (34.8)		6 (26.1)	28 (24.8)	
≧50	14 (63.6)	88 (65.2)	0.89	17 (73.9)	85 (75.2)	0.89
Stage†						
1-3	15 (68.2)	115 (85.2)		17 (73.9)	94 (83.2)	
4	7 (31.8)	20 (14.8)	0.07[F]	6 (26.1)	19 (16.8)	0.37[F]
Histology						
Mucinous adenocarcinoma	2 (9.1)	5 (3.7)		1 (4.4)	2 (1.8)	
Not Mucinous adenocarcinoma	20 (90.9)	130 (96.3)	0.25[F]	22 (95.7)	110 (98.2)	0.43[F]
Tumor grade						
Low	19 (86.4)	124 (91.9)		20 (87.0)	106 (93.8)	
High	2 (9.1)	6 (4.4)	0.31[F]	3 (13.0)	7 (6.2)	0.37[F]
Missing	1 (4.5)	5 (3.7)		0 (0.0)	0 (0.0)	
Primary tumor side††						
Left-sided and rectum	12 (54.6)	98 (72.6)		11 (47.8)	79 (30.1)	
Right-sided	10 (45.5)	37 (27.4)	0.13	12 (52.2)	34 (69.9)	**0.04**
RAS						
Wild type	10 (45.5)	89 (65.9)		18 (78.3)	69 (61.1)	
Mutation	12 (54.6)	42 (31.1)	**0.04**	5 (21.7)	43 (38.1)	0.13
Missing	0 (0.0)	4 (3.0)		0 (0.0)	1 (0.9)	
BRAF V600E						
Wild type	14 (63.6)	127 (94.1)		12 (52.2)	111 (98.2)	
Mutation	7 (31.8)	3 (2.2)	**<0.01**[F]	11 (47.8)	1 (0.9)	**<0.01**[F]
Missing	1 (4.5)	5 (3.7)		0 (0.0)	1 (0.9)	
MSI						
Low/stable	16 (72.7)	125 (92.6)		15 (65.2)	104 (92.0)	
High	6 (27.3)	8 (5.9)	**<0.01**[F]	8 (34.8)	9 (8.0)	**<0.01**[F]
Missing	0 (0.0)	2 (1.5)		0 (0.0)	0 (0.0)	

Abbreviations: CIMP, CpG island methylator phenotype; OR, odds ratio; CI, confidence interval; MSI, microsatellite instability.

[F]Fisher's exact test.

doi:10.6342/NTU202300311

Table 7. Distribution of CIMP-high or CIMP-low/negative according to risk factors of CRC stratified by gender. Logistic regression was used for statistical analysis[3].

Variable, N (%)		Male				Female			
		CIMP-high CRC (N =14)	CIMP-low/negative CRC (N =75)	OR (95% CI) high vs. low/negative	*p*-value	CIMP-high CRC (N = 31)	CIMP-low/negative CRC (N = 173)	OR (95% CI) high vs. low/negative	*p*-value
Family history									
	None	21 (95.5)	113 (83.7)	reference		21 (91.3)	105 (92.9)	reference	
	Yes	1 (4.6)	22 (16.3)	0.25 (0.03-1.91)	0.18	2 (8.7)	8 (7.08)	1.25 (0.25-6.31)	0.79
Colorectal polyp									
	0	16 (72.7)	110 (82.7)	reference		16 (69.6)	99 (88.4)	reference	
	≥ 1	6 (27.3)	23 (17.3)	1.79 (0.63-5.08)	0.27	7 (30.4)	13 (11.6)	3.33 (1.16-9.62)	**0.03**
BMI (kg/m2) at diagnosis, WHO criteria									
	< 25	13 (59.1)	78 (57.8)	reference		16 (69.6)	85 (75.2)	reference	
	25-29	7 (31.8)	49 (36.3)	0.857	0.76	7 (30.4)	21 (18.6)	1.771	0.27
	≥ 30	2 (9.1)	8 (5.9)	1.500	0.63	0 (0.0)	7 (6.2)	NA	NA
BMI (kg/m^2) at diagnosis									
	< 27.5	17 (77.3)	109 (80.7)	reference		20 (87.0)	96 (85.0)	reference	
	≥ 27.5	5 (22.7)	26 (19.3)	1.233	0.70	3 (13.0)	17 (15.0)	0.847	0.80
DM									
	None	17 (77.3)	114 (85.1)	reference		20 (87.0)	87 (77.0)	reference	
	Yes	5 (22.7)	20 (14.9)	1.68 (0.56-2.06)	0.36	3 (13.0)	26 (23.0)	0.50 (0.14-1.82)	0.30
Hyperlipidemia									
	None	16 (72.7)	104 (77.0)	reference		15 (65.2)	85 (75.2)	reference	
	Yes	6 (27.3)	31 (23.0)	1.26 (0.45-3.497)	0.66	8 (34.8)	28 (24.8)	1.62 (0.62-4.22)	0.32
NSAIDs use									
	None	21 (95.5)	128 (94.8)	reference		20 (87.0)	106 (94.6)	reference	
	Yes	1 (4.6)	7 (5.2)	0.87 (0.10-7.44)	0.90	3 (13.0)	6 (5.4)	2.65 (0.61-11.48)	0.19
HRT									
	None	22 (100.0)	135 (100.0)	reference		23 (100.0)	108 (96.4)	reference	

doi:10.6342/NTU202300311

	Yes	0 (0.0)	0 (0.0)	NA	NA	0 (0.0)	4 (3.6)	NA	0.98

Abbreviations: CIMP, CpG island methylator phenotype; OR, odds ratio; CI, confidence interval; BMI, body mass index; DM, diabetes mellitus; NSAIDs, non-steroidal anti-inflammatory drugs; HRT, hormone replacement therapy; WHO, world health organization.

doi:10.6342/NTU202300311

Table 8. Clinicopathological features in patients with *BRAF V600E*-mutated colorectal cancer[124].

Characteristic	*De novo* metastatic MSS, N= 54 (100%)
Age (years)	
Median	51
Range	26-79
Sex	
Male	30 (55.6)
Female	24 (44.4)
Stage	
1-3	0 (0)
4	54 (100)
Histology	
Adenocarcinoma†	54 (100)
Mucinous adenocarcinoma	0 (0)
Tumor grade	
Low	43 (79.6)
High	10 (18.5)
Missing	1 (1.9)
Location of primary tumor	
Left-sided	20 (37.0)
Right-sided	34 (63.0)
Metastatic site	
Liver-limited	14 (25.9)
Peritoneum	23 (42.6)
First-line chemotherapy	
Triplet	8 (14.8)
Doublet	41 (75.9)
Fluoropyrimidine monotherapy	3 (5.6)
No	2 (3.7)
First-line targeted therapy	
Bevacizumab	29 (53.7)
Cetuximab	8 (14.8)

Abbreviations: MSS: microsatellite stable; NA: not available

†One patient had adenocarcinoma rich in signet ring cells.

doi:10.6342/NTU202300311

Table 9. Immune cells in Cox proportional hazard model for hazard ratios of progression-free survival and overall survival in patients with *de novo* metastatic MSS *BRAF V600E*-mutated CRC[124].

	Progression-free survival		Overall survival	
Immune cell	HR (95% CI)	*p* -value	HR (95% CI)	*p* -value
B cell	0.72 (0.52-0.98)	0.039	1.08 (0.78-1.50)	0.631
CD4 T cell	0.61 (0.43-0.86)	0.005	0.83 (0.59-1.16)	0.276
CD8 T cell	1.03 (0.77-1.39)	0.842	0.96 (0.68-1.37)	0.832
Cytotoxic cell	1.19 (0.89-1.59)	0.251	1.01 (0.75-1.37)	0.937
Dendritic cell	1.19 (0.86-1.64)	0.290	1.41 (0.98-2.02)	0.061
Exhausted CD8	1.11 (0.82-1.51)	0.500	1.08 (0.77-1.52)	0.653
Macrophage	1.14 (0.87-1.47)	0.340	1.11 (0.84-1.48)	0.463
Mast cell	0.99 (0.71-1.37)	0.944	1.20 (0.87-1.67)	0.270
Neutrophil	1.08 (0.81-1.43)	0.602	1.05 (0.76-1.44)	0.781
NK CD56dim cell	1.05 (0.74-1.48)	0.793	1.06 (0.75-1.52)	0.725
NK cell	1.05 (0.79-1.38)	0.746	1.15 (0.86-1.55)	0.350
T cell	0.91 (0.66-1.25)	0.552	0.90 (0.64-1.26)	0.536
Th1 cell	1.03 (0.76-1.40)	0.848	0.99 (0.71-1.38)	0.968
Treg	0.90 (0.64-1.27)	0.538	0.98 (0.73-1.32)	0.918

Abbreviation: CI: confidence interval; HR: hazard ratio. NK: natural killer; Th1: T helper 1; Treg: T regulatory cell

doi:10.6342/NTU202300311

Table 10. Immune checkpoints link to B and T cell signaling in Cox proportional hazard model for hazard ratios of progression-free survival and overall survival in patients with *de novo* metastatic MSS *BRAF V600E*-mutated CRC[124].

	Progression-free survival		Overall survival	
Checkpoints	HR (95% CI)	*p*-value	HR (95% CI)	*p*-value
CD40LG	0.73 (0.49-1.10)	0.136	0.62 (0.43-0.89)	0.01
CD40	1.12 (0.81-1.56)	0.503	1.61 (0.87-1.56)	0.319
CD80	1.09 (0.78-1.51)	0.631	1.01 (0.75-1.36)	0.946
CD86	1.1 (0.81-1.50)	0.541	1.11 (0.84-1.47)	0.476
ICOS	0.92 (0.68-1.24)	0.589	0.71 (0.51-0.977)	0.035
ICOSLG	0.69 (0.49-0.97)	0.034	1.03 (0.73-1.45)	0.888
CD274	1.25 (0.87-1.77)	0.224	1.19 (0.86-1.66)	0.301
PDCD1	0.81 (0.56-1.18)	0.273	0.93 (0.68-1.28)	0.661
CD28	0.93 (0.63-1.37)	0.705	0.99 (0.72-1.39)	0.992
CTLA4	0.82 (0.6-1.12)	0.215	0.74 (0.53-1.04)	0.086

Abbreviation: CI: confidence interval; HR: hazard ratio.

doi:10.6342/NTU202300311

Table 11. Complement genes in the Cox proportional hazards model for hazard ratios of progression-free survival and overall survival in patients with *de novo* metastatic MSS *BRAF V600E* mutant CRC[124].

	Progression-free survival		Overall survival	
Complement genes	HR (95% CI)	*p* -value	HR (95% CI)	*p* -value
Classical pathway				
C1S	1.54 (1.10, 2.14)	0.010	1.18 (0.81, 1.72)	0.378
C1R	1.46 (1.03, 2.06)	0.030	1.15 (0.77, 1.70)	0.490
C1QA	1.35 (0.99, 1.84)	0.050	1.52 (1.04, 2.22)	0.029
C1QB	1.33 (0.98, 1.80)	0.062	1.37 (0.97, 1.91)	0.068
C1QBP	0.84 (0.62, 1.14)	0.279	0.85 (0.60, 1.19)	0.352
C2	1.00 (0.75, 1.32)	0.984	1.28 (0.96, 1.70)	0.090
C4B	1.00 (0.74, 1.35)	0.971	1.06 (0.77, 1.44)	0.732
Lectin pathway				
MBL2	1.26 (0.93, 1.72)	0.129	1.46 (1.04, 2.04)	0.027
MASP1	1.09 (0.78, 1.43)	0.507	1.24 (0.73, 1.45)	0.154
MASP2	0.76 (0.54, 1.05)	0.106	0.96 (0.65, 1.40)	0.845
Alternative pathway				
CFB	0.93 (0.69, 1.26)	0.679	1.07 (0.77, 1.46)	0.684
CFD	0.75 (0.54, 1.03)	0.077	1.02 (0.76, 1.37)	0.875
Complement regulators				
CD46	0.93 (0.69, 1.26)	0.657	0.82 (0.58, 1.15)	0.264
CD55	0.97 (0.70, 1.34)	0.876	0.68 (0.46, 1.00)	0.053
CFI	1.20 (0.91, 1.60)	0.187	1.02 (0.75, 1.39)	0.884
CFP	1.01 (0.53, 1.03)	0.967	0.78 (0.65, 1.41)	0.226
SERPING1	1.64 (1.18, 2.27)	0.003	1.20 (0.83, 1.72)	0.331
CD59	1.09 (0.82, 1.45)	0.537	1.47 (1.61, 2.02)	0.020
CR1	1.01 (0.69, 1.46)	0.976	1.54 (0.51, 1.17)	0.009
C4BPA	0.68 (0.84, 1.44)	0.013	0.92 (0.92, 1.66)	0.611
Terminal pathway				
C3	1.28 (0.91, 1.79)	0.147	1.29 (0.87, 1.90)	0.198
C5	1.24 (0.90, 1.70)	0.181	1.01 (0.74, 1.32)	0.925
C6	1.06 (0.68, 1.18)	0.701	1.03 (0.66, 1.25)	0.851
C7	1.19 (0.87, 1.63)	0.250	0.90 (0.62, 1.27)	0.538
C8A	1.11 (0.81, 1.54)	0.493	1.00 (0.65, 1.52)	0.988
C8B	0.92 (0.63, 1.35)	0.696	0.86 (0.55, 1.32)	0.497
C9	0.89 (0.65, 1.24)	0.521	0.96 (0.67, 1.36)	0.834
Complement receptors				
ITGB2	0.99 (0.73, 1.33)	0.957	1.11 (0.80, 1.52)	0.518
ITGAX	0.90 (0.68, 1.18)	0.458	0.91 (0.66, 1.25)	0.563
ITGAM	1.13 (0.86, 1.49)	0.364	1.16 (0.86, 1.55)	0.334
C3AR1	1.07 (0.81, 1.41)	0.617	1.27 (0.93, 1.71)	0.119
CR2	0.74 (0.50, 0.92)	0.081	0.96 (0.65, 1.28)	0.829

Abbreviation: CI: confidence interval; CRC: colorectal cancer. HR: hazard ratio. OS: overall survival. PFS: progression-free survival.

doi:10.6342/NTU202300311

Table 12. Univariate and multivariate analyses through a Cox proportional hazards model for hazard ratios of progression-free survival and overall survival in patients with *de novo* metastatic MSS *BRAF V600E* mutant CRC[124].

	Progression-free survival				Overall survival			
Variable	Univariate analysis		Multivariate analysis		Univariate analysis		Multivariate analysis	
	HR (95% CI)	*p* -value	HR (95% CI)	*p* -value (BH correction)	HR (95% CI)	*p* -value	HR (95% CI)	*p* -value (BH correction)
Complement score (High)	1.91 (1.06-3.44))	0.032	1.62 (0.88-2.98)	0.123 (0.123)	2.35 (1.24-4.48)	0.009	2.44 (1.26-4.70)	0.008 (0.008)
Sex (Male)	1.56 (0.85-2.97)	0.15			1.18 (0.62-2.23)	0.61		
Primary tumor site (Right)	0.81 (0.42-1.56)	0.52			0.97 (0.48-1.99)	0.94		
Tumor grade (High)	1.90 (0.86-4.17)	0.11			4.52 (1.99-10.3)	< 0.001	5.00 (2.14-11.7)	< 0.001 (0.002)
Liver-limited metastasis	0.90 (0.49-1.63)	0.72			1.04 (0.55-1.98)	0.89		
Peritoneum metastasis	0.83 (0.35-1.99)	0.68			0.42 (0.15-1.22)	0.11		
First-line chemotherapy doublet vs. fluoropyrimidine monotherapy	2.14 (1.10-4.14)	0.02	2.08 (1.03-4.17)	0.040 (0.067)	1.24 (0.61-2.49)	0.55		
First-line chemotherapy triplet vs. fluoropyrimidine monotherapy	0.81 (0.44-1.49)	0.50			1.05 (0.56-1.99)	0.88		
First-line targeted therapy – Bevacizumab	0.37 (0.11-1.25)	0.11	0.28 (0.08-1.00)	0.050 (0.067)	0.44 (0.13-1.48)	0.18		
First-line targeted therapy–Cetuximab	0.26 (0.06-1.08)	0.063	0.20 (0.05-0.90)	0.035 (0.067)	0.37 (0.09-1.60)	0.18		

Abbreviation: CI: confidence interval; CRC: colorectal cancer. HR: hazard ratio. MSS: microsatellite stable. OS: overall survival. PFS: progression-free survival. BH:

doi:10.6342/NTU202300311

Benjamini & Hochberg multiple testing correction method

doi:10.6342/NTU202300311

References

1. Sung H, Ferlay J, Siegel RL, Laversanne M, Soerjomataram I, Jemal A *et al.* Global Cancer Statistics 2020: GLOBOCAN Estimates of Incidence and Mortality Worldwide for 36 Cancers in 185 Countries. *CA: Cancer J Clin* 2021; **71**(3): 209-249; doi https://doi.org/10.3322/caac.21660.
2. Arnold M, Abnet CC, Neale RE, Vignat J, Giovannucci EL, McGlynn KA *et al.* Global Burden of 5 Major Types of Gastrointestinal Cancer. *Gastroenterology* 2020; **159**(1): 335-349.e315; doi 10.1053/j.gastro.2020.02.068.
3. Chen KH, Lin LI, Yuan CT, Tseng LH, Chao YL, Liang YH *et al.* Association between risk factors, molecular features and CpG island methylator phenotype colorectal cancer among different age groups in a Taiwanese cohort. *Br J Cancer* 2021; **125**(1): 48-54; doi 10.1038/s41416-021-01300-5.
4. Health Promotion Administration, Ministry of Health Welfare. Taiwan Cancer Registry Statistical Service (1980-2019). Available at: https://twcr.tw/?page_id=1657. Accessed on 8 Nov. 2022.
5. Brenner H, Kloor M, Pox CP. Colorectal cancer. *Lancet* 2014; **383**(9927): 1490-1502; doi 10.1016/s0140-6736(13)61649-9.
6. Taylor DP, Burt RW, Williams MS, Haug PJ, Cannon-Albright LA. Population-based family history-specific risks for colorectal cancer: a constellation approach. *Gastroenterology* 2010; **138**(3): 877-885; doi 10.1053/j.gastro.2009.11.044.
7. Jess T, Rungoe C, Peyrin-Biroulet L. Risk of colorectal cancer in patients with ulcerative colitis: a meta-analysis of population-based cohort studies. *Clin Gastroenterol Hepatol* 2012; **10**(6): 639-645; e-pub ahead of print 2012/02/01; doi 10.1016/j.cgh.2012.01.010.
8. Bollati V, Baccarelli A. Environmental epigenetics. *Heredity (Edinb)* 2010; **105**(1): 105-112; e-pub ahead of print 2010/02/25; doi 10.1038/hdy.2010.2.
9. Hughes LA, van den Brandt PA, Goldbohm RA, de Goeij AF, de Bruine AP, van Engeland

doi:10.6342/NTU202300311

M *et al.* Childhood and adolescent energy restriction and subsequent colorectal cancer risk: results from the Netherlands Cohort Study. *Int J Epidemiol* 2010; **39**(5): 1333-1344; doi 10.1093/ije/dyq062.

10. Hughes LA, van den Brandt PA, de Bruine AP, Wouters KA, Hulsmans S, Spiertz A *et al.* Early life exposure to famine and colorectal cancer risk: a role for epigenetic mechanisms. *PloS one* 2009; **4**(11): e7951; e-pub ahead of print 2009/12/04; doi 10.1371/journal.pone.0007951.

11. Lea AJ, Altmann J, Alberts SC, Tung J. Resource base influences genome-wide DNA methylation levels in wild baboons (Papio cynocephalus). *Molecular Ecology* 2016; **25**(8): 1681-1696; doi 10.1111/mec.13436.

12. Chen KH, Lai LC, Lin LI, Chang HF, Chao YL, Lin BR *et al.* Abstract 4382: Epigenetic deregulation in glycolysis genes for colorectal cancer. *Cancer Res* 2019; **79**(13_Supplement): 4382-4382; doi 10.1158/1538-7445.Am2019-4382.

13. McCubrey JA, Steelman LS, Chappell WH, Abrams SL, Wong EW, Chang F *et al.* Roles of the Raf/MEK/ERK pathway in cell growth, malignant transformation and drug resistance. *Biochim Biophys Acta* 2007; **1773**(8): 1263-1284; doi 10.1016/j.bbamcr.2006.10.001.

14. Santarpia L, Lippman SM, El-Naggar AK. Targeting the MAPK-RAS-RAF signaling pathway in cancer therapy. *Expert Opin Ther Targets* 2012; **16**(1): 103-119; doi 10.1517/14728222.2011.645805.

15. Douillard JY, Oliner KS, Siena S, Tabernero J, Burkes R, Barugel M *et al.* Panitumumab-FOLFOX4 treatment and RAS mutations in colorectal cancer. *N Engl J Med* 2013; **369**(11): 1023-1034; doi 10.1056/NEJMoa1305275.

16. Heinemann V, von Weikersthal LF, Decker T, Kiani A, Vehling-Kaiser U, Al-Batran SE *et al.* FOLFIRI plus cetuximab versus FOLFIRI plus bevacizumab as first-line treatment for patients with metastatic colorectal cancer (FIRE-3): a randomised, open-label, phase 3 trial.

doi:10.6342/NTU202300311

Lancet Oncol 2014; **15**(10): 1065-1075; doi 10.1016/s1470-2045(14)70330-4.

17. Van Cutsem E, Lenz H-J, Köhne C-H, Heinemann V, Tejpar S, Melezínek I *et al.* Fluorouracil, Leucovorin, and Irinotecan Plus Cetuximab Treatment and RAS Mutations in Colorectal Cancer. *J Clin Oncol* 2015; **33**(7): 692-700; doi 10.1200/JCO.2014.59.4812.

18. Cremolini C, Loupakis F, Antoniotti C, Lupi C, Sensi E, Lonardi S *et al.* FOLFOXIRI plus bevacizumab versus FOLFIRI plus bevacizumab as first-line treatment of patients with metastatic colorectal cancer: updated overall survival and molecular subgroup analyses of the open-label, phase 3 TRIBE study. *Lancet Oncol* 2015; **16**(13): 1306-1315; doi 10.1016/s1470-2045(15)00122-9.

19. Modest DP, Ricard I, Heinemann V, Hegewisch-Becker S, Schmiegel W, Porschen R *et al.* Outcome according to KRAS-, NRAS- and BRAF-mutation as well as KRAS mutation variants: pooled analysis of five randomized trials in metastatic colorectal cancer by the AIO colorectal cancer study group. *Ann Oncol* 2016; **27**(9): 1746-1753; doi 10.1093/annonc/mdw261.

20. Schirripa M, Cremolini C, Loupakis F, Morvillo M, Bergamo F, Zoratto F *et al.* Role of NRAS mutations as prognostic and predictive markers in metastatic colorectal cancer. *Int J Cancer* 2015; **136**(1): 83-90; doi 10.1002/ijc.28955.

21. Davies H, Bignell GR, Cox C, Stephens P, Edkins S, Clegg S *et al.* Mutations of the BRAF gene in human cancer. *Nature* 2002; **417**(6892): 949-954; doi 10.1038/nature00766.

22. Tran B, Kopetz S, Tie J, Gibbs P, Jiang ZQ, Lieu CH *et al.* Impact of BRAF Mutation and Microsatellite Instability on the Pattern of Metastatic Spread and Prognosis in Metastatic Colorectal Cancer. *Cancer* 2011; **117**(20): 4623-4632; doi 10.1002/cncr.26086.

23. Tol J, Nagtegaal ID, Punt CJ. BRAF mutation in metastatic colorectal cancer. *N Engl J Med* 2009; **361**(1): 98-99; doi 10.1056/NEJMc0904160.

24. De Roock W, Claes B Fau - Bernasconi D, Bernasconi D Fau - De Schutter J, De Schutter J

doi:10.6342/NTU202300311

Fau - Biesmans B, Biesmans B Fau - Fountzilas G, Fountzilas G Fau - Kalogeras KT *et al.* Effects of KRAS, BRAF, NRAS, and PIK3CA mutations on the efficacy of cetuximab plus chemotherapy in chemotherapy-refractory metastatic colorectal cancer: a retrospective consortium analysis. *Lancet Oncol* 2010; **11**(8).753-762

25. Jones JC, Renfro LA, Al-Shamsi HO, Schrock AB, Rankin A, Zhang BY *et al.* (Non-V600) BRAF Mutations Define a Clinically Distinct Molecular Subtype of Metastatic Colorectal Cancer. *J Clin Oncol* 2017; **35**(23): 2624-2630; doi 10.1200/jco.2016.71.4394.

26. Tsai JH, Liau JY, Lin YL, Tseng LH, Lin LI, Yeh KH *et al.* Frequent BRAF mutation in early-onset colorectal cancer in Taiwan: association with distinct clinicopathological and molecular features and poor clinical outcome. *J Clin Pathol* 2016; **69**(4): 319-325; doi 10.1136/jclinpath-2015-203335.

27. Chen KH, Lin YL, Liau JY, Tsai JH, Tseng LH, Lin LI *et al.* BRAF mutation may have different prognostic implications in early- and late-stage colorectal cancer. *Med Oncol* 2016; **33**(5): 39; doi 10.1007/s12032-016-0756-6.

28. Vilar E, Gruber SB. Microsatellite instability in colorectal cancer-the stable evidence. *Nat Rev Clin Oncol* 2010; **7**(3): 153-162; doi 10.1038/nrclinonc.2009.237.

29. Cancer Genome Atlas N. Comprehensive molecular characterization of human colon and rectal cancer. *Nature* 2012; **487**(7407): 330-337; doi 10.1038/nature11252.

30. Parsons R, Li GM, Longley MJ, Fang WH, Papadopoulos N, Jen J *et al.* Hypermutability and mismatch repair deficiency in RER+ tumor cells. *Cell* 1993; **75**(6): 1227-1236

31. Gryfe R, Kim H, Hsieh ET, Aronson MD, Holowaty EJ, Bull SB *et al.* Tumor microsatellite instability and clinical outcome in young patients with colorectal cancer. *N Engl J Med* 2000; **342**(2): 69-77; doi 10.1056/nejm200001133420201.

32. Popat S, Hubner R, Houlston RS. Systematic review of microsatellite instability and colorectal cancer prognosis. *J Clin Oncol* 2005; **23**(3): 609-618; doi

doi:10.6342/NTU202300311

10.1200/jco.2005.01.086.

33. Llosa NJ, Cruise M, Tam A, Wicks EC, Hechenbleikner EM, Taube JM *et al.* The vigorous immune microenvironment of microsatellite instable colon cancer is balanced by multiple counter-inhibitory checkpoints. *Cancer Discov* 2015; **5**(1): 43-51; doi 10.1158/2159-8290.CD-14-0863.

34. Schwitalle Y, Kloor M, Eiermann S, Linnebacher M, Kienle P, Knaebel HP *et al.* Immune response against frameshift-induced neopeptides in HNPCC patients and healthy HNPCC mutation carriers. *Gastroenterology* 2008; **134**(4): 988-997; doi 10.1053/j.gastro.2008.01.015.

35. Le DT, Uram JN, Wang H, Bartlett BR, Kemberling H, Eyring AD *et al.* PD-1 Blockade in Tumors with Mismatch-Repair Deficiency. *N Engl J Med* 2015; **372**(26): 2509-2520; doi 10.1056/NEJMoa1500596.

36. Le DT, Durham JN, Smith KN, Wang H, Bartlett BR, Aulakh LK *et al.* Mismatch-repair deficiency predicts response of solid tumors to PD-1 blockade. *Science* 2017; doi 10.1126/science.aan6733.

37. Overman MJ, McDermott R, Leach JL, Lonardi S, Lenz HJ, Morse MA *et al.* Nivolumab in patients with metastatic DNA mismatch repair-deficient or microsatellite instability-high colorectal cancer (CheckMate 142): an open-label, multicentre, phase 2 study. *Lancet Oncology* 2017; **18**(9): 1182-1191.

38. FDA grants accelerated approval to pembrolizumab for first tissue/site agnostic indication.

39. Andre T, Shiu KK, Kim TW, Jensen BV, Jensen LH, Punt C *et al.* Pembrolizumab in Microsatellite-Instability-High Advanced Colorectal Cancer. *N Engl J Med*; **383**(23): 2207-2218; doi 10.1056/NEJMoa2017699.

40. Mandal R, Samstein RM, Lee KW, Havel JJ, Wang H, Krishna C *et al.* Genetic diversity of tumors with mismatch repair deficiency influences anti-PD-1 immunotherapy response.

doi:10.6342/NTU202300311

Science 2019; **364**(6439): 485-491; doi 10.1126/science.aau0447.

41. Lu C, Guan J, Lu S, Jin Q, Rousseau B, Lu T *et al.* DNA Sensing in Mismatch Repair-Deficient Tumor Cells Is Essential for Anti-tumor Immunity. *Cancer Cell* 2021; **39**(1): 96-108.e106; doi 10.1016/j.ccell.2020.11.006.

42. Cercek A, Lumish M, Sinopoli J, Weiss J, Shia J, Lamendola-Essel M *et al.* PD-1 Blockade in Mismatch Repair–Deficient, Locally Advanced Rectal Cancer. *N Engl J Med* **386**(25): 2363-2376; doi 10.1056/NEJMoa2201445.

43. M. Chalabi1 YLV, J. van den Berg3, K. Sikorska4, G. Beets5, A.V. Lent6, M.C. Grootscholten2, A. Aalbers5, N. Buller7, H. Marsman8, E. Hendriks9, P.W.A. Burger10, T. Aukema11, S. Oosterling12, R. Beets-Tan13, T.N. Schumacher14, M. van Leerda. LBA7 - Neoadjuvant immune checkpoint inhibition in locally advanced MMR-deficient colon cancer: The NICHE-2 study. *Ann Oncol 2022; **33** (suppl_7): S808-S869 101016/annonc/annonc1089* 2022.

44. Jung G, Hernandez-Illan E, Moreira L, Balaguer F, Goel A. Epigenetics of colorectal cancer: biomarker and therapeutic potential. *Nat Rev Gastroenterol Hepatol* 2020; **17**(2): 111-130; doi 10.1038/s41575-019-0230-y.

45. Toyota M, Ahuja N, Ohe-Toyota M, Herman JG, Baylin SB, Issa JP. CpG island methylator phenotype in colorectal cancer. *PNAS* 1999; **96**(15): 8681-8686;

46. Toyota M, Ohe-Toyota M, Ahuja N, Issa JP. Distinct genetic profiles in colorectal tumors with or without the CpG island methylator phenotype. *PNAS* 2000; **97**(2): 710-715;

47. Samowitz WS, Albertsen H, Herrick J, Levin TR, Sweeney C, Murtaugh MA *et al.* Evaluation of a large, population-based sample supports a CpG island methylator phenotype in colon cancer. *Gastroenterology* 2005; **129**(3): 837-845; doi 10.1053/j.gastro.2005.06.020.

48. Ogino S, Cantor M, Kawasaki T, Brahmandam M, Kirkner GJ, Weisenberger DJ *et al.* CpG island methylator phenotype (CIMP) of colorectal cancer is best characterised by

doi:10.6342/NTU202300311

quantitative DNA methylation analysis and prospective cohort studies. *Gut* 2006; **55**(7): 1000-1006; doi 10.1136/gut.2005.082933.

49. Weisenberger DJ, Siegmund KD, Campan M, Young J, Long TI, Faasse MA *et al.* CpG island methylator phenotype underlies sporadic microsatellite instability and is tightly associated with BRAF mutation in colorectal cancer. *Nat genet* 2006; **38**(7): 787-793; doi 10.1038/ng1834.

50. Hughes LA, Khalid-de Bakker CA, Smits KM, van den Brandt PA, Jonkers D, Ahuja N *et al.* The CpG island methylator phenotype in colorectal cancer: progress and problems. *Biochimica et Biophysica Acta* 2012; **1825**(1): 77-85; e-pub ahead of print 2011/11/08; doi 10.1016/j.bbcan.2011.10.005.

51. Juo YY, Johnston FM, Zhang DY, Juo HH, Wang H, Pappou EP *et al.* Prognostic value of CpG island methylator phenotype among colorectal cancer patients: a systematic review and meta-analysis. *Ann Oncol* 2014; **25**(12): 2314-2327; doi 10.1093/annonc/mdu149.

52. Gallois C, Laurent-Puig P, Taieb J. Methylator phenotype in colorectal cancer: A prognostic factor or not? *Crit Rev Oncol/Hematol* 2016; **99**: 74-80; doi 10.1016/j.critrevonc.2015.11.001.

53. Chen KH, Lin LI, Tseng LH, Lin YL, Liau JY, Tsai JH *et al.* CpG Island Methylator Phenotype May Predict Poor Overall Survival of Patients with Stage IV Colorectal Cancer. *Oncology* 2019; **96**(3): 156-163; doi 10.1159/000493387.

54. Bruni D, Angell HK, Galon J. The immune contexture and Immunoscore in cancer prognosis and therapeutic efficacy. *Nat Rev Cancer* 2020; **20**(11): 662-680; doi 10.1038/s41568-020-0285-7.

55. Fridman WH, Pages F, Sautes-Fridman C, Galon J. The immune contexture in human tumours: impact on clinical outcome. *Nat Rev Cancer* 2012; **12**(4): 298-306; doi 10.1038/nrc3245.

doi:10.6342/NTU202300311

56. Pagès F, Berger A, Camus M, Sanchez-Cabo F, Costes A, Molidor R *et al.* Effector Memory T Cells, Early Metastasis, and Survival in Colorectal Cancer. *N Engl J Med* 2005; **353**(25): 2654-2666; doi 10.1056/NEJMoa051424.

57. Galon J, Costes A, Sanchez-Cabo F, Kirilovsky A, Mlecnik B, Lagorce-Pagès C *et al.* Type, density, and location of immune cells within human colorectal tumors predict clinical outcome. *Science* 2006; **313**(5795): 1960-1964; doi 10.1126/science.1129139.

58. Mlecnik B, Tosolini M, Kirilovsky A, Berger A, Bindea G, Meatchi T *et al.* Histopathologic-based prognostic factors of colorectal cancers are associated with the state of the local immune reaction. *J Clin Oncol* 2011; **29**(6): 610-618; doi 10.1200/jco.2010.30.5425.

59. Pagès F, Mlecnik B, Marliot F, Bindea G, Ou FS, Bifulco C *et al.* International validation of the consensus Immunoscore for the classification of colon cancer: a prognostic and accuracy study. *Lancet* 2018; **391**(10135): 2128-2139; doi 10.1016/s0140-6736(18)30789-x.

60. Marliot F, Chen X, Kirilovsky A, Sbarrato T, El Sissy C, Batista L *et al.* Analytical validation of the Immunoscore and its associated prognostic value in patients with colon cancer. *J Immunother Cancer* 2020; **8**(1); doi 10.1136/jitc-2019-000272.

61. Bindea G, Mlecnik B, Tosolini M, Kirilovsky A, Waldner M, Obenauf AC *et al.* Spatiotemporal dynamics of intratumoral immune cells reveal the immune landscape in human cancer. *Immunity* 2013; **39**(4): 782-795; doi 10.1016/j.immuni.2013.10.003.

62. Melero I, Rouzaut A, Motz GT, Coukos G. T-cell and NK-cell infiltration into solid tumors: a key limiting factor for efficacious cancer immunotherapy. *Cancer Discov* 2014; **4**(5): 522-526; doi 10.1158/2159-8290.Cd-13-0985.

63. Vayrynen JP, Haruki K, Lau MC, Vayrynen SA, Zhong R, Dias Costa A *et al.* The Prognostic Role of Macrophage Polarization in the Colorectal Cancer Microenvironment. *Cancer Immunol Res* 2021; **9**(1): 8-19; doi 10.1158/2326-6066.CIR-20-0527.

doi:10.6342/NTU202300311

64. Weisenberger DJ, Levine AJ, Long TI, Buchanan DD, Walters R, Clendenning M *et al.* Association of the colorectal CpG island methylator phenotype with molecular features, risk factors, and family history. *Cancer Epidemiol, Biomarkers & Pre* 2015; **24**(3): 512-519; doi 10.1158/1055-9965.epi-14-1161.

65. Alegria-Torres JA, Baccarelli A, Bollati V. Epigenetics and lifestyle. *Epigenomics* 2011; **3**(3): 267-277; doi 10.2217/epi.11.22.

66. consultations We. Appropriate body-mass index for Asian populations and its implications for policy and intervention strategies. *Lancet* 2004; **363**(9403): 157-163; doi 10.1016/s0140-6736(03)15268-3.

67. Liu J, Tang L, Yi J, Li G, Lu Y, Xu Y *et al.* Unique characteristics of CpG island methylator phenotype (CIMP) in a Chinese population with colorectal cancer. *BMC Gastroenterology* 2019; **19**(1): 173; doi 10.1186/s12876-019-1086-x.

68. Lee S, Cho NY, Yoo EJ, Kim JH, Kang GH. CpG island methylator phenotype in colorectal cancers: comparison of the new and classic CpG island methylator phenotype marker panels. *Arch Pathol Lab Med* 2008; **132**(10): 1657-1665; doi 10.1043/1543-2165(2008)132[1657:cimpic]2.0.co;2.

69. Samowitz WS, Albertsen H, Sweeney C, Herrick J, Caan BJ, Anderson KE *et al.* Association of smoking, CpG island methylator phenotype, and V600E BRAF mutations in colon cancer. *J Natl Cancer Inst* 2006; **98**(23): 1731-1738; doi 10.1093/jnci/djj468.

70. Hughes LA, Simons CC, van den Brandt PA, Goldbohm RA, de Goeij AF, de Bruine AP *et al.* Body size, physical activity and risk of colorectal cancer with or without the CpG island methylator phenotype (CIMP). *PloS one* 2011; **6**(4): e18571; doi 10.1371/journal.pone.0018571.

71. Maegawa S, Lu Y, Tahara T, Lee JT, Madzo J, Liang S *et al.* Caloric restriction delays age-related methylation drift. *Nat Commun* 2017; **8**(1): 539; doi 10.1038/s41467-017-00607-3.

doi:10.6342/NTU202300311

72. Horvath S. DNA methylation age of human tissues and cell types. *Genome Biol* 2013; **14**(10): R115-R115; doi 10.1186/gb-2013-14-10-r115.

73. Wang T, Maden SK, Luebeck GE, Li CI, Newcomb PA, Ulrich CM *et al.* Dysfunctional epigenetic aging of the normal colon and colorectal cancer risk. *Clin Epigenetics* 2020; **12**(1): 5; doi 10.1186/s13148-019-0801-3.

74. de Toro-Martín J, Guénard F, Tchernof A, Hould F-S, Lebel S, Julien F *et al.* Body mass index is associated with epigenetic age acceleration in the visceral adipose tissue of subjects with severe obesity. *Clin Epigenetics* 2019; **11**(1): 172-172; doi 10.1186/s13148-019-0754-6.

75. Nevalainen T, Kananen L, Marttila S, Jylhava J, Mononen N, Kahonen M *et al.* Obesity accelerates epigenetic aging in middle-aged but not in elderly individuals. *Clin Epigenetics* 2017; **9**: 20; doi 10.1186/s13148-016-0301-7.

76. Amitay EL, Carr PR, Jansen L, Roth W, Alwers E, Herpel E *et al.* Smoking, alcohol consumption and colorectal cancer risk by molecular pathological subtypes and pathways. *Br J Cancer* 2020; **122**(11): 1604-1610; doi 10.1038/s41416-020-0803-0.

77. Clarke CN, Kopetz ES. BRAF mutant colorectal cancer as a distinct subset of colorectal cancer: clinical characteristics, clinical behavior, and response to targeted therapies. J Gastrointest Oncol 2015; **6**(6):660-667. doi: 10.3978/j.issn.2078-6891.2015.077.

78. Guinney J, Dienstmann R, Wang X, de Reyniès A, Schlicker A, Soneson C *et al.* The consensus molecular subtypes of colorectal cancer. *Nat Med* 2015; **21**(11): 1350-1356; doi 10.1038/nm.3967.

79. Barras D, Missiaglia E, Wirapati P, Sieber OM, Jorissen RN, Love C *et al.* BRAF V600E Mutant Colorectal Cancer Subtypes Based on Gene Expression. *Clin Can.Res* 2017; **23**(1): 104-115; doi 10.1158/1078-0432.ccr-16-0140.

80. Kopetz S, Murphy DA, Pu J, Ciardiello F, Desai J, Grothey A *et al.* Molecular correlates of

doi:10.6342/NTU202300311

clinical benefit in previously treated patients (pts) with BRAF V600E-mutant metastatic colorectal cancer (mCRC) from the BEACON study. *J Clin Oncol* 2021; **39**(15_suppl): 3513-3513; doi 10.1200/JCO.2021.39.15_suppl.3513.

81. Van Cutsem E, Kohne CH, Lang I, Folprecht G, Nowacki MP, Cascinu S *et al.* Cetuximab plus irinotecan, fluorouracil, and leucovorin as first-line treatment for metastatic colorectal cancer: updated analysis of overall survival according to tumor KRAS and BRAF mutation status. *J Clin Oncol* 2011; **29**(15): 2011-2019; doi 10.1200/jco.2010.33.5091.

82. Richman SD, Seymour MT, Chambers P, Elliott F, Daly CL, Meade AM *et al.* KRAS and BRAF mutations in advanced colorectal cancer are associated with poor prognosis but do not preclude benefit from oxaliplatin or irinotecan: results from the MRC FOCUS trial. *J Clin Oncol* 2009; **27**(35): 5931-5937; doi 10.1200/jco.2009.22.4295.

83. Cohen R, Liu H, Fiskum J, Adams R, Chibaudel B, Maughan TS *et al.* BRAFV600E Mutation in First-line Metastatic Colorectal Cancer: an Analysis of Individual Patient Data from the ARCAD Database. *J Natl Cancer Inst* 2021; doi 10.1093/jnci/djab042.

84. Robert C. A decade of immune-checkpoint inhibitors in cancer therapy. *Nat Commu* 2020; **11**(1): 3801; doi 10.1038/s41467-020-17670-y.

85. Yarchoan M, Hopkins A, Jaffee EM. Tumor Mutational Burden and Response Rate to PD-1 Inhibition. *N Engl J Med* 2017; **377**(25): 2500-2501; doi 10.1056/NEJMc1713444.

86. André T, Shiu K-K, Kim TW, Jensen BV, Jensen LH, Punt C *et al.* Pembrolizumab in Microsatellite-Instability–High Advanced Colorectal Cancer. *N Engl J Med* 2020; **383**(23): 2207-2218; doi 10.1056/NEJMoa2017699.

87. Overman MJ, McDermott R, Leach JL, Lonardi S, Lenz H-J, Morse MA *et al.* Nivolumab in patients with metastatic DNA mismatch repair-deficient or microsatellite instability-high colorectal cancer (CheckMate 142): an open-label, multicentre, phase 2 study. *Lancet Oncology* 2017; **18**(9): 1182-1191; doi 10.1016/S1470-2045(17)30422-9.

doi:10.6342/NTU202300311

88. Morris VK, Parseghian CM, Escano M, Johnson B, Raghav KPS, Dasari A *et al.* Phase I/II trial of encorafenib, cetuximab, and nivolumab in patients with microsatellite stable, BRAFV600E metastatic colorectal cancer. *J Clin Oncol* 2022; **40**(4_suppl): 12-12; doi 10.1200/JCO.2022.40.4_suppl.012.

89. Tabernero J, Ros J, Elez E. The Evolving Treatment Landscape in BRAF-V600E-Mutated Metastatic Colorectal Cancer. *Am Soc Clin Oncol Educ Book* 2022; **42**: 1-10; doi 10.1200/EDBK_349561.

90. Hsu CL, Ou DL, Bai LY, Chen CW, Lin L, Huang SF *et al.* Exploring Markers of Exhausted CD8 T Cells to Predict Response to Immune Checkpoint Inhibitor Therapy for Hepatocellular Carcinoma. *Liver Cancer* 2021; doi 10.1159/000515305.

91. Robinson MD, McCarthy DJ, Smyth GK. edgeR: a Bioconductor package for differential expression analysis of digital gene expression data. *Bioinformatics* 2010; **26**(1): 139-140; doi 10.1093/bioinformatics/btp616.

92. Roumenina LT, Daugan MV, Petitprez F, Sautes-Fridman C, Fridman WH. Context-dependent roles of complement in cancer. *Nat Rev Cancer* 2019; **19**(12): 698-715; doi 10.1038/s41568-019-0210-0.

93. Danaher P, Warren S, Dennis L, D'Amico L, White A, Disis ML *et al.* Gene expression markers of Tumor Infiltrating Leukocytes. *J ImmunoTher Cancer* 2017; **5**(1): 18; doi 10.1186/s40425-017-0215-8.

94. Newman AM, Liu CL, Green MR, Gentles AJ, Feng W, Xu Y *et al.* Robust enumeration of cell subsets from tissue expression profiles. *Nat Methods* 2015; **12**(5): 453-457; doi 10.1038/nmeth.3337.

95. Azizi E, Carr AJ, Plitas G, Cornish AE, Konopacki C, Prabhakaran S *et al.* Single-Cell Map of Diverse Immune Phenotypes in the Breast Tumor Microenvironment. *Cell* 2018; **174**(5): 1293-1308.e1236; doi https://doi.org/10.1016/j.cell.2018.05.060.

doi:10.6342/NTU202300311

96. Liu J, Lichtenberg T, Hoadley KA, Poisson LM, Lazar AJ, Cherniack AD *et al.* An Integrated TCGA Pan-Cancer Clinical Data Resource to Drive High-Quality Survival Outcome Analytics. *Cell* 2018; **173**(2): 400-416.e411; doi 10.1016/j.cell.2018.02.052.

97. Hause RJ, Pritchard CC, Shendure J, Salipante SJ. Classification and characterization of microsatellite instability across 18 cancer types. *Nat Med* 2016; **22**(11): 1342-1350; doi 10.1038/nm.4191.

98. Marisa L, de Reyniès A, Duval A, Selves J, Gaub MP, Vescovo L *et al.* Gene Expression Classification of Colon Cancer into Molecular Subtypes: Characterization, Validation, and Prognostic Value. *PLOS Med* 2013; **10**(5): e1001453; doi 10.1371/journal.pmed.1001453.

99. Murata K, Baldwin WM. Mechanisms of complement activation, C4d deposition, and their contribution to the pathogenesis of antibody-mediated rejection. *Transplant Rev* 2009; **23**(3): 139-150; doi https://doi.org/10.1016/j.trre.2009.02.005.

100. Kolev M, Le Friec G, Kemper C. Complement--tapping into new sites and effector systems. *Nat Rev Immunol* 2014; **14**(12): 811-820; doi 10.1038/nri3761.

101. Kemper C, Köhl J. Back to the future - non-canonical functions of complement. *Semin Immunol* 2018; **37**: 1-3; e-pub ahead of print 2018/06/03; doi 10.1016/j.smim.2018.05.002.

102. Medler TR, Murugan D, Horton W, Kumar S, Cotechini T, Forsyth AM *et al.* Complement C5a Fosters Squamous Carcinogenesis and Limits T Cell Response to Chemotherapy. *Cancer Cell* 2018; **34**(4): 561-578.e566; doi 10.1016/j.ccell.2018.09.003.

103. Nitta H, Murakami Y, Wada Y, Eto M, Baba H, Imamura T. Cancer cells release anaphylatoxin C5a from C5 by serine protease to enhance invasiveness. *Oncol Rep* 2014; **32**(4): 1715-1719; doi 10.3892/or.2014.3341.

104. Ajona D, Ortiz-Espinosa S, Pio R, Lecanda F. Complement in Metastasis: A Comp in the Camp. *Front Immunol* 2019; **10**(669); doi 10.3389/fimmu.2019.00669.

105. Markiewski MM, DeAngelis RA, Benencia F, Ricklin-Lichtsteiner SK, Koutoulaki A,

doi:10.6342/NTU202300311

Gerard C *et al.* Modulation of the antitumor immune response by complement. *Nat Immunol* 2008; **9**(11): 1225-1235; doi 10.1038/ni.1655.

106. Bonavita E, Gentile S, Rubino M, Maina V, Papait R, Kunderfranco P *et al.* PTX3 Is an Extrinsic Oncosuppressor Regulating Complement-Dependent Inflammation in Cancer. *Cell* 2015; **160**(4): 700-714; doi 10.1016/j.cell.2015.01.004.

107. Nabizadeh JA, Manthey HD, Steyn FJ, Chen W, Widiapradja A, Md Akhir FN *et al.* The Complement C3a Receptor Contributes to Melanoma Tumorigenesis by Inhibiting Neutrophil and CD4⁺ T Cell Responses. *J Immunol* 2016: 1600210; doi 10.4049/jimmunol.1600210.

108. Cohen D, Colvin Rb Fau - Daha MR, Daha Mr Fau - Drachenberg CB, Drachenberg Cb Fau - Haas M, Haas M Fau - Nickeleit V, Nickeleit V Fau - Salmon JE *et al.* Pros and cons for C4d as a biomarker. *Kidney int* 2012;**81** (7): 628-639

109. Ajona D, Pajares MJ, Corrales L, Perez-Gracia JL, Agorreta J, Lozano MD *et al.* Investigation of complement activation product c4d as a diagnostic and prognostic biomarker for lung cancer. *J Natl Cancer Inst* 2013; **105**(18): 1385-1393; doi 10.1093/jnci/djt205.

110. Daugan MV, Revel M, Russick J, Dragon-Durey M-A, Gaboriaud C, Robe-Rybkine T *et al.* Complement C1s and C4d as Prognostic Biomarkers in Renal Cancer: Emergence of Noncanonical Functions of C1s. *Cancer Immunol Res* 2021; **9**(8): 891; doi 10.1158/2326-6066.CIR-20-0532.

111. Roumenina LT, Daugan MV, Noe R, Petitprez F, Vano YA, Sanchez-Salas R *et al.* Tumor Cells Hijack Macrophage-Produced Complement C1q to Promote Tumor Growth. *Cancer Immunol Res* 2019; **7**(7): 1091-1105; doi 10.1158/2326-6066.CIR-18-0891.

112. Edin S, Wikberg ML, Dahlin AM, Rutegard J, Oberg A, Oldenborg PA *et al.* The distribution of macrophages with a M1 or M2 phenotype in relation to prognosis and the

doi:10.6342/NTU202300311

molecular characteristics of colorectal cancer. *PLoS One* 2012; **7**(10): e47045; doi 10.1371/journal.pone.0047045.

113. Ajona D, Ortiz-Espinosa S, Moreno H, Lozano T, Pajares MJ, Agorreta J *et al.* A Combined PD-1/C5a Blockade Synergistically Protects against Lung Cancer Growth and Metastasis. *Cancer Discov* 2017; **7**(7): 694-703; doi 10.1158/2159-8290.CD-16-1184.

114. Pyonteck SM, Akkari L Fau - Schuhmacher AJ, Schuhmacher Aj Fau - Bowman RL, Bowman Rl Fau - Sevenich L, Sevenich L Fau - Quail DF, Quail Df Fau - Olson OC *et al.* CSF-1R inhibition alters macrophage polarization and blocks glioma progression. Nat Med 2013;19(10):1264-1272. doi: 10.1038/nm.3337.

115. Razak AR, Cleary JM, Moreno V, Boyer M, Calvo Aller E, Edenfield W *et al.* Safety and efficacy of AMG 820, an anti-colony-stimulating factor 1 receptor antibody, in combination with pembrolizumab in adults with advanced solid tumors. *J Immunother Cancer* 2020; **8**(2); doi 10.1136/jitc-2020-001006.

116. Sung H, Siegel RL, Rosenberg PS, Jemal A. Emerging cancer trends among young adults in the USA: analysis of a population-based cancer registry. *Lancet Public Health* 2019; **4**(3): e137-e147; doi 10.1016/s2468-2667(18)30267-6.

117. Bailey CE, Hu C-Y, You YN, Bednarski BK, Rodriguez-Bigas MA, Skibber JM *et al.* Increasing Disparities in the Age-Related Incidences of Colon and Rectal Cancers in the United States, 1975-2010. *JAMA Surgery* 2015; **150**(1): 17-22; doi 10.1001/jamasurg.2014.1756.

118. Pearlman R, Frankel WL, Swanson B, Zhao W, Yilmaz A, Miller K *et al.* Prevalence and Spectrum of Germline Cancer Susceptibility Gene Mutations Among Patients With Early-Onset Colorectal Cancer. *JAMA Oncol* 2017; **3**(4): 464-471; doi 10.1001/jamaoncol.2016.5194.

119. Garrett WS. The gut microbiota and colon cancer. *Science* 2019; **364**(6446): 1133-1135; doi

doi:10.6342/NTU202300311

10.1126/science.aaw2367.

120. Tjalsma H, Boleij A, Marchesi JR, Dutilh BE. A bacterial driver–passenger model for colorectal cancer: beyond the usual suspects. *Nat Rev Microbiol* 2012; **10**(8): 575-582; doi 10.1038/nrmicro2819.

121. Ternes D, Karta J, Tsenkova M, Wilmes P, Haan S, Letellier E. Microbiome in Colorectal Cancer: How to Get from Meta-omics to Mechanism? *Trends Microbiol* 2020; **28**(5): 401-423; doi 10.1016/j.tim.2020.01.001.

122. Yang Y, Du L, Shi D, Kong C, Liu J, Liu G *et al.* Dysbiosis of human gut microbiome in young-onset colorectal cancer. *Nat Commun* 2021; **12**(1): 6757; doi 10.1038/s41467-021-27112-y.

123. Walker SP, Tangney M, Claesson MJ. Sequence-Based Characterization of Intratumoral Bacteria—A Guide to Best Practice. *Front Oncol* 2020; **10**; doi 10.3389/fonc.2020.00179.

124. Chen K-H, Hsu C-L, Su Y-L, Yuan C-T, Lin L-I, Tsai J-H *et al.* Novel prognostic implications of complement activation in the tumour microenvironment for de novo metastatic BRAF V600E mutant colorectal cancer. *Br J Cancer* 2022; doi 10.1038/s41416-022-02010-2.

125. Frade R, Rodrigues-Lima F, Huang S, Xie K, Guillaume N, Bar-Eli M. Procathepsin-L, a Proteinase that Cleaves Human C3 (the Third Component of Complement), Confers High Tumorigenic and Metastatic Properties to Human Melanoma Cells1. *Cancer Res* 1998; **58**(13): 2733-2736.

126. Reddel CJ, Tan CW, Chen VM. Thrombin Generation and Cancer: Contributors and Consequences. *Cancers (Basel)* 2019; **11**(1); doi 10.3390/cancers11010100.

127. Zha H, Han X, Zhu Y, Yang F, Li Y, Li Q *et al.* Blocking C5aR signaling promotes the anti-tumor efficacy of PD-1/PD-L1 blockade. *Oncoimmunology* 2017; **6**(10): e1349587; doi 10.1080/2162402X.2017.1349587.

doi:10.6342/NTU202300311

128. Risitano AM, Peffault de Latour R, Marano L, Frieri C. Discovering C3 targeting therapies for paroxysmal nocturnal hemoglobinuria: Achievements and pitfalls. *Semin Immunol* 2022: 101618; doi 10.1016/j.smim.2022.101618.

129. Ostrem JM, Peters U, Sos ML, Wells JA, Shokat KM. K-Ras(G12C) inhibitors allosterically control GTP affinity and effector interactions. *Nature* 2013; **503**(7477): 548-551; doi 10.1038/nature12796.

130. Hong DS, Fakih MG, Strickler JH, Desai J, Durm GA, Shapiro GI *et al.* KRASG12C Inhibition with Sotorasib in Advanced Solid Tumors. *N Engl J Med* 2020; **383**(13): 1207-1217; doi 10.1056/NEJMoa1917239.

131. Fakih MG, Kopetz S, Kuboki Y, Kim TW, Munster PN, Krauss JC *et al.* Sotorasib for previously treated colorectal cancers with KRAS(G12C) mutation (CodeBreaK100): a prespecified analysis of a single-arm, phase 2 trial. *Lancet Oncol* 2022; **23**(1): 115-124; doi 10.1016/S1470-2045(21)00605-7.

132. Health Promotion Administration, Ministry of Health Welfare. Taiwan Cancer Registry Statistical Service (1980-2017). Available at: http://tcr.cph.ntu.edu.tw/main.php?Page=A5B2(Chinese). Accessed on 20 Aug. 2020.

doi:10.6342/NTU202300311

Appendix

I. Representative works of doctoral thesis. (The published articles are listed in the following pages)

1. Chen, KH., Lin, LI., Yuan, CT. et al. Association between risk factors, molecular features and CpG island methylator phenotype colorectal cancer among different age groups in a Taiwanese cohort. *Br J Cancer* 2021;**125**, 48–54; https://doi.org/10.1038/s41416-021-01300-5

2. Chen KH, Hsu CL, Su YL, Yuan CT, Lin LI, Tsai JH, Liang YH, Cheng AL, Yeh KH. Novel prognostic implications of complement activation in the tumor microenvironment for *de novo* metastatic *BRAF V600E* mutant colorectal cancer. *Br J Cancer* 2022. https://doi: 10.1038/s41416-022-02010-2

II. The other works of colorectal cancer in recent years.

1. Liang YH, Chen KH, Tsai JH, Cheng YM, Lee CC, Kao CH, Chan KY, Chen YT, Hsu WL, Yeh KH. Proteasome inhibitors restore the STAT1 pathway and enhance the expression of MHC class I on human colon cancer cells. *J Biomed Sci.* 2021;**28(1)**:75; https://doi: 10.1186/s12929-021-00769-9.
2. Liang YH, Tsai JH, Cheng YM, Chan KY, Hsu WL, Lee CC, Chen KH, Yeh KH. Chemotherapy agents stimulate dendritic cells against human colon cancer cells through upregulation of the transporter associated with antigen processing. *Sci Rep.* 2021;**11(1)**:9080; doi: 10.1038/s41598-021-88648-z.
3. Chen KH, Lin LI, Tseng LH, Lin YL, Liau JY, Tsai JH, Liang JT, Lin BR, Cheng AL, Yeh KH. CpG Island Methylator Phenotype May Predict Poor Overall Survival of Patients with Stage IV Colorectal Cancer. *Oncology.* 2019;**96(3)**:156-163; doi: 10.1159/000493387.
4. Chen KH, Lai LC, Lin LI, Chang HF, Chao YL, Lin BR, Liang JT, Cheng AL, Chuang Eric Y,

doi:10.6342/NTU202300311

Yeh KH. Abstract 4382: Epigenetic deregulation in glycolysis genes for colorectal cancer. *Cancer Research* 2019; **79**(13_Supplement): 4382-4382; doi 10.1158/1538-7445.Am2019-4382.

5. Chen KH, Shao YY, Chen HM, Lin YL, Lin ZZ, Lai MS, Cheng AL, Yeh KH. Primary tumor site is a useful predictor of cetuximab efficacy in the third-line or salvage treatment of *KRAS* wild-type (exon 2 non-mutant) metastatic colorectal cancer: a nationwide cohort study. *BMC Cancer.* 2016;**16(1)**:327.
6. Chen KH, Lin YL, Liau JY, Tsai JH, Tseng LH, Lin LI, Liang JT, Lin BR, Hung JS, Chang YL, Yeh KH, Cheng AL. *BRAF* mutation may have different prognostic implications in early- and late-stage colorectal cancer. *Med Oncol.* 2016;**33(5)**:39 ; doi 10.1007/s12032-016-0756-6.
7. Chen KH, Shao YY, Yeh YC, Shau WY, Kuo Raymond NC, Lin ZZ, Chen HM, Yeh KH, Cheng AL, Lai MS. Association of Diabetes Mellitus with Increased Mortality in Patients Receiving Curative Surgery for Colon Cancer. *Oncologist.* 2014 Sep;**19(9)**:951-8.

doi:10.6342/NTU202300311